

Fluorescent Reporter Proteins

Robert E. Campbell and Michael W. Davidson

INTRODUCTION

For more than a decade the growing class of fluorescent proteins (FPs) defined as homologues of *Aequorea victoria* green FP (avGFP), which are capable of forming an intrinsic chromophore, has almost single-handedly launched and fueled a new era in cell biology. These powerful research tools provide investigators with a means of fusing a genetically encoded optical probe to any one of a practically unlimited variety of protein targets to examine living systems using fluorescence microscopy and related methodology (see Figure 1.1; for recent reviews, see references [1–4]). The diverse array of practical applications for FPs ranges from targeted markers for organelles and other subcellular structures, to protein fusions designed to monitor mobility and dynamics, to reporters of transcriptional regulation (Figure 1.2). FPs have also opened the door to creating highly specific biosensors for live-cell imaging of numerous intracellular phenomena, including pH and ion concentration fluctuations, protein kinase activity, apoptosis, voltage, cyclic nucleotide signaling, and tracing neuronal pathways [5–9]. In addition, by applying selected promoters and targeting signals, FP biosensors can be introduced into an intact organism and directed to specific tissues, cell types, and subcellular compartments to enable monitoring a variety of physiological processes using fluorescence resonance energy transfer (FRET) techniques.

If FPs are the “fuel” for the live-cell imaging revolution, the “engines” are the technical advances in widefield fluorescence and confocal microscopes. Some notable advances include low light level digital charge coupled device (CCD) cameras as well as spinning-disk and swept-field instruments. As of today, avGFP and its color-shifted variants, in conjunction with sophisticated imaging equipment, have demonstrated invaluable service in many thousands of live-cell imaging experiments. One of the most important features of FPs is that they are minimally invasive for living cells, especially compared to

many traditional synthetic fluorophores (that are often toxic or photoreactive). The relatively low or nonexistent toxicity of FPs (when expressed at low levels relative to endogenous proteins) permits visualization and recording of time-lapse image sequences for extended periods of time [10, 11]. As we will discuss in this chapter, continued advances in FP engineering technology have enabled the fine-tuning of critical fluorescent imaging parameters, including brightness, spectral profiles, photostability, maturation time, and pH insensitivity, to provide a stream of new and advanced probes for optical microscopy. These structural and functional enhancements have stimulated a wide variety of investigations into protein dynamics and function using FP chimeras imaged at low light intensities for many hours to extract valuable biochemical information.

Today we take the exceptional and revolutionary utility of FPs for granted, and it may be hard for some researchers to imagine research without them. It is therefore somewhat surprising that more than 30 years had to pass between the first scientific report of the isolation of avGFP [12] and its first application as a tool for biological imaging [13]. The first report of fluorescence in the bioluminescent hydrozoan jellyfish species *Aequorea victoria* was recorded more than 60 years ago [14] and a protein extract was independently demonstrated by two investigators to be responsible for this “green” fluorescence in the 1960s and 1970s [12, 15]. It took several more decades to identify the responsible protein, clone the gene encoding the protein, and elucidate the primary amino acid structure [16]. In light of the time span between the original discovery and cloning of avGFP, it is rather remarkable that only 2 years later, an image revealing the fluorescent sensory neurons of the nematode highlighted with the same jellyfish protein was featured on the cover of the journal *Science* [13]. This landmark event unambiguously demonstrated the utility of avGFP as a genetic marker in cells evolutionarily far removed from hydrozoans and ushered in a new

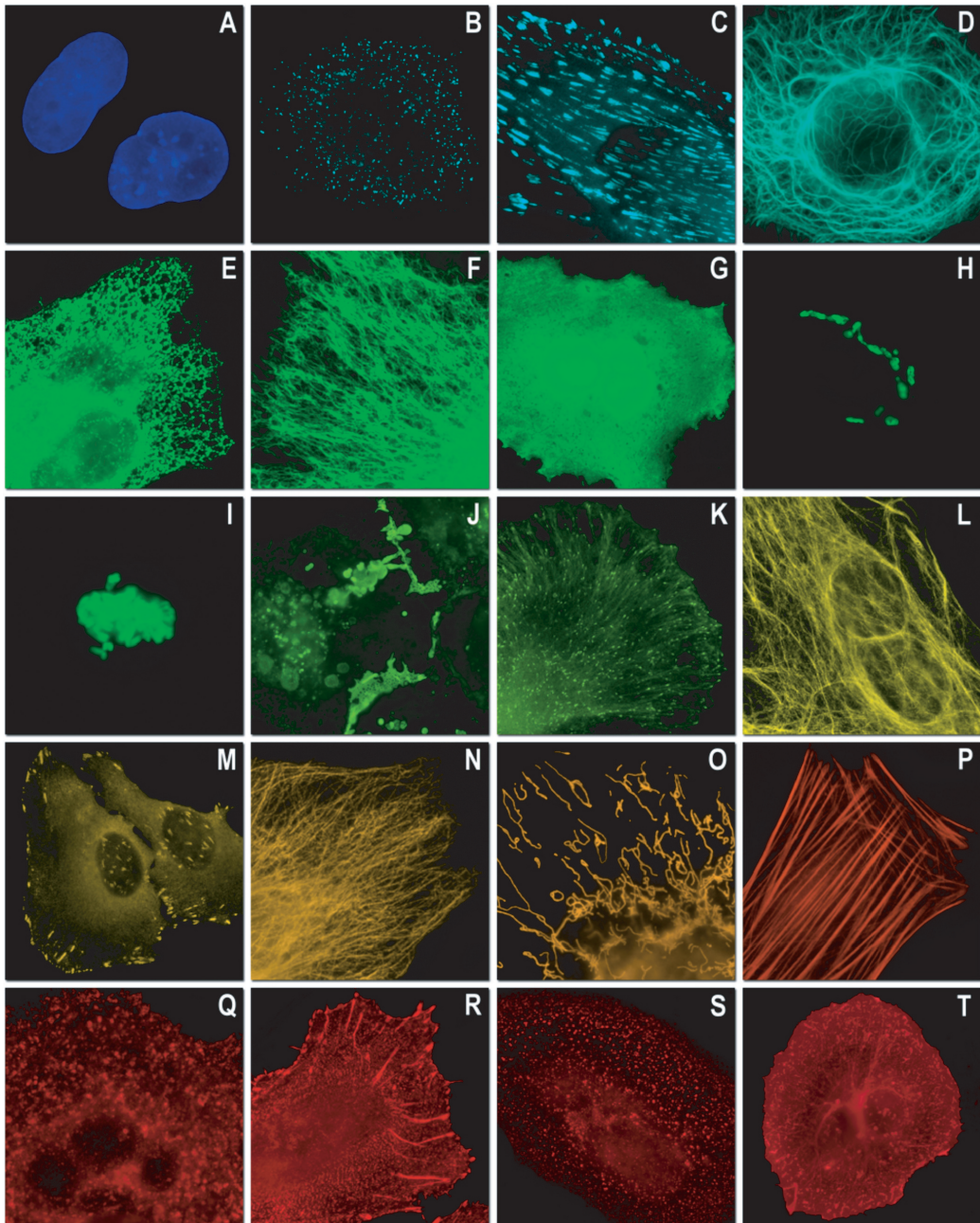


Figure 1.1. Subcellular localization of selected FP fusions (listed in Table 1.1) with targeting proteins imaged in widefield fluorescence. Images are pseudocolored to match the FP emission profile. The FP fusion terminus and number of linker amino acids is indicated after the name of the targeted organelle or fusion protein. The fusion protein and host cell line is given in parentheses (A) EBFP2-lamin-B1-N-10 (human lamin B1; nuclear envelope; HeLa); (B) ECFP-peroxisomes-C-2 (peroximal targeting signal 1; PTS1; HeLa); (C) mCerulean-vinculin-C-23 (human; focal adhesions; Fox Lung); (D) mTFP1-keratin-N-17 (human cytokeratin 18; intermediate filaments; HeLa); (E) EGFP-endoplasmic reticulum-N-3 (calreticulin signal sequence and KDEL retention sequence; HeLa); (F) mEmerald-vimentin-N-7 (human vimentin; intermediate filaments; HeLa); (G) mAzami Green-N1 (cloning vector; whole cell fluorescence; HeLa); (H) Superfolder avGFP-Golgi-N-7 (N-terminal 81 amino acids of human β -1,4-galactosyltransferase; Golgi complex; HeLa); (I) mT-Sapphire-H2B-N-6 (human histone H2B; metaphase; HeLa); (J) mVenus-Cx43-N-7 (rat α -1 connexin-43; gap junctions; HeLa); (K) YPet-EB3-N-7 (human microtubule-associated protein; RP/EB family; Fox Lung); (L) mKusabira Orange-vimentin-N-7 (human; intermediate filaments; Opossum Kidney); (M) tdTomato-paxillin-N-22 (chicken; focal adhesions; Fox Lung); (N) TagRFP-tubulin-C-6 (human α -tubulin; microtubules; HeLa); (O) DsRed2-mitochondria-N-7 (human cytochrome C oxidase subunit VIII; mitochondria; HeLa); (P) mStrawberry-actin-C-7 (human β -actin; filamentous actin; Fox Lung); (Q) mRFP1-lysosomes-C-20 (rat lysosomal membrane glycoprotein 1; HeLa); (R) mCherry- α -actinin-N-19 (human nonmuscle; cytoskeleton; HeLa); (S) mKate-clathrin light chain-C-15 (human; clathrin vesicles; HeLa); (T) mPlum-farnesyl-C-5 (20-amino acid farnesylation signal from c-Ha-Ras; plasma membrane; HeLa).

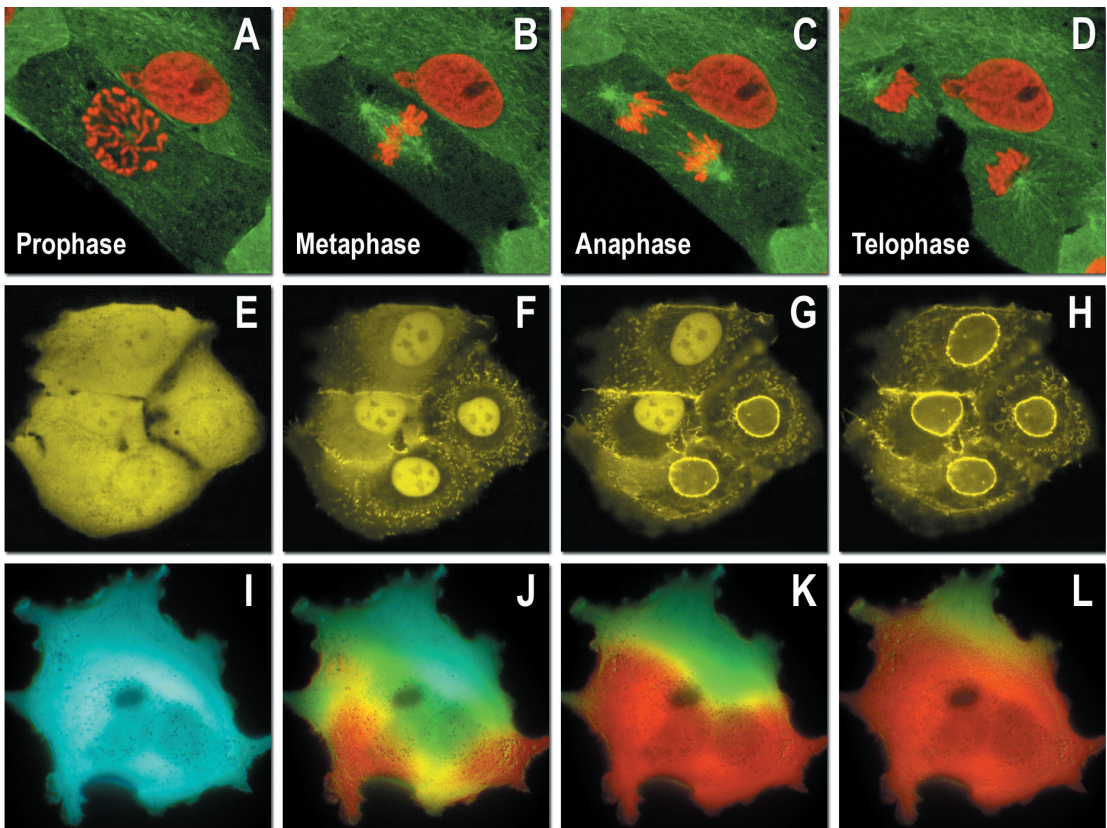


Figure 1.2. Fluorescent protein reporters in action imaged with spinning disk confocal and widefield microscopy. **A–D:** Observing mitosis in dual-labeled normal pig kidney (LLC-PK1 cell line) epithelial cells stably expressing mCherry-H2B-N-6 (histones) and mEmerald-EB3-N-7 (microtubule + end binding protein), **(A)** A cell in prophase (lower) is captured adjacent to a cell in interphase, $t = 0$; **(B)** The lower cell forms a spindle and enters metaphase. Note the EB3 patterns emanating from the spindle poles and traversing to the plasma and nuclear membranes, $t = 20$ min; **(C)** During anaphase, the spindle poles translocate to opposite sides of the cell, pulling the condensed chromosomes along, $t = 60$ min; **(D)** The chromosomes begin to decondense during telophase as the daughter cells recover from cell division (midbody not visible). **E–H:** Spinning disk confocal images selected from a time-lapse series of human cervical adenocarcinoma (HeLa cell line) epithelial cells expressing mKusabira Orange-annexin (A4)-C-12 during ionomycin-induced translocation to the plasma and nuclear membranes, **(E)** A cluster of four cells exhibits expression of the chimera throughout the nucleus and cytoplasm $t = 0$, ionomycin ($10 \mu\text{M}$) added; **(F)** Shortly after addition of ionomycin, the annex chimera begins to translocate to the plasma membrane, clearly revealing the nuclei, $t = 3$ min; **(G)** The annex chimera migrates to the membrane in two of the nuclei, time = 5 min; **(H)** The nuclear membranes of all four nuclei display translocated annex chimera, time = 7 min. **(I–L)** Widefield fluorescence calcium imaging in the cytosol of HeLa cells expressing the circularly permuted cameleon YC3.60; **(I)** Real color image of a single cell, $t = 0$, histamine ($10 \mu\text{M}$) added; **(J)** Pseudo-colored ratio image of the HeLa cell as a calcium wave initiates at the two loci on the membrane, $t = 10$ sec; **(K)** The calcium wave propagates through the cytoplasm, $t = 10.5$ sec; **(L)** The calcium wave reaches the distant portion of the cell, $t = 11.0$ sec.

era in biological fluorescence imaging. Through the mid-1990s, a number of genetic variants of the original avGFP nucleotide sequence were developed that featured enhanced green fluorescence (EGFP) [17] and altered fluorescence emission spectral profiles in the blue (BFP) [18, 19], cyan (CFP) [20], and yellow (YFP) [21] regions of the visible spectrum. Perhaps the single most significant advance following the initial cloning and early mutagenesis efforts on wild-type avGFP was the discovery of cyan, green, yellow, orange, and red-fluorescing avGFP homologues in nonbioluminescent reef corals and sea anemones [22]. This discovery not

only provided a source of new FPs with new emission colors but also demonstrated that this protein motif can potentially occur in a wide range of classes and species.

FPs have now been discovered in organisms ranging from marine invertebrates to crustaceans and probably exist in many other species [23–26]. In fact, a protein known as nidogen [27], found tucked away in basement membrane of all mammals, has been characterized to have a domain consisting of an 11-stranded β -barrel remarkably similar to the three-dimensional structure of avGFP, despite having only 10% sequence homology.

In nidogen, the amino acid triplet Ile-Gly-Gly (IGG) replaces the chromophore-forming residues Ser-Tyr-Gly (SYG) found in avGFP. In addition, several other residues critical for the generation of a functional chromophore in FPs have been replaced in nidogen by residues that eliminate the possibility of fluorescence. Nevertheless, the β -barrel structure appears to have been evolutionarily conserved for a variety of purposes other than fluorescence, and nature may surprise us again with new sources of chromoproteins and FPs in species previously not considered.

In this chapter, we discuss the basic properties of FPs, including brightness, photostability, color class, oligomerization, folding, and maturation efficiency, and then compare them among themselves and to alternative technologies. In addition, we discuss recent advances in protein engineering strategies as well as improvements to the FP color palette and the development of the current armament of photoactivatable FPs. Finally, we provide suggestions for the best FP choices in single- and multicolor imaging and potential avenues for obtaining the genes encoding these proteins.

COMPARING FLUORESCENT PROTEINS WITH ALTERNATIVE FLUOROPHORES

The single most important advantage of FPs over traditional organic fluorophores and the newer semiconductor quantum dot probes is their widespread compatibility with tissues and intact organisms. In the crowded environment of the cell interior there are thousands of proteins, each with a unique shape, function, and concentration. From the perspective of the cell, expression of the gene encoding an FP (or FP chimera) adds one more relatively benign protein (a perfectly disguised spy!) into this crowded environment. In contrast, a synthetic fluorophore or quantum dot is an unfamiliar and conspicuous entity inside the cell or organism. For example, many synthetic fluorophores are hydrophobic and may bind to exposed hydrophobic patches on other proteins or intercalate into DNA. Furthermore, an FP is created inside the cell from transcription and translation of a gene artificially introduced into the cell's genome. In contrast, synthetic fluorophores and quantum dots are made outside the cell (probably on the lab bench of a chemist) and must breach the cell membrane to reach the cytoplasm, possibly to the detriment of the cell or organism. Other important advantages of FPs include their ability to specifically target fluorescent probes in subcellular compartments and the extremely low or absent levels of phototoxicity. Among the disadvantages of fluorescent proteins are artifacts introduced by delivery of the exogenous nucleic acid, often manifested in high levels of autofluorescence produced by transfection reagents. Overexpression of fluorescent proteins is also a concern

but can be offset by careful selection of clones that stably express the fusion products, at appropriate levels.

The advantages of FPs mentioned previously render them the clear and obvious technology of choice for the study of intracellular protein localization and dynamics in living cells or organisms. Simply put, the fact that FPs are *proteins* and are thus *genetically encoded* is an overwhelming advantage relative to all other fluorescent technologies. However, secondary considerations may or may not impact the choice of technology for certain applications, and these will be addressed in the following paragraphs. A number of reviews comparing synthetic dyes, quantum dots, and FP technology have been published in recent years [28–31]. The following sections, rather than repeating the relative merits of each approach, will focus only on some of the most important issues viewed from an FP-centric perspective.

Brightness

The brightness of a fluorophore is proportional to the product of the fluorescence quantum yield (QY) and the extinction coefficient (EC). The EC (units of $\text{M}^{-1} \text{cm}^{-1}$) describes how effective a molecule is at absorbing light, whereas the QY (a ratio with no units) is the fraction of the absorbed photons subsequently reemitted as fluorescence. By definition, QY values must lie somewhere between 0 (no fluorescence) and 1 (every absorbed photon is emitted as fluorescence). It is not particularly informative to consider either EC or QY in isolation because the actual fluorescent brightness is proportional to the product of these two values. To put some perspective on relative fluorescent brightness, we will arbitrarily pick two fluorophores useful in live- and fixed-cell imaging, one of which is bright and one of which is relatively dim. The bright fluorophore is sulforhodamine 101 (the sulfonyl chloride form of which is known as Texas Red), which has a fluorescent brightness of $125 \text{ mM}^{-1} \text{ cm}^{-1}$ (i.e., $139,000 \text{ M}^{-1} \text{ cm}^{-1} * 0.9$) [32]. Note that the units for brightness are arbitrarily provided here as $\text{mM}^{-1} \text{ cm}^{-1}$ (as opposed to $\text{M}^{-1} \text{ cm}^{-1}$ for EC). The relatively dim fluorophore is the cell tracker dye Lucifer yellow CH, which has a fluorescent brightness of $5 \text{ mM}^{-1} \text{ cm}^{-1}$ ($24,200 \text{ M}^{-1} \text{ cm}^{-1} * 0.21$) [32]. Nominally, this brightness range of 5 to $125 \text{ mM}^{-1} \text{ cm}^{-1}$ is an intuitive and convenient yardstick by which to compare different fluorophores. Due to their high ECs and exceptional QYs [33], quantum dots produce brightness values that typically fall into the range of 100–1000 $\text{mM}^{-1} \text{ cm}^{-1}$, depending on excitation wavelength.

In a head-to-head comparison of the brightness of fluorescein and EGFP, two fluorophores with similar excitation and emission wavelength profiles, fluorescein comes out the winner. The brightness of fluorescein ($69 \text{ mM}^{-1} \text{ cm}^{-1}$) is about double that of EGFP ($34 \text{ mM}^{-1} \text{ cm}^{-1}$) [3]. This single comparison nicely

represents a general trend in comparison of the brightness of FPs and synthetic dyes; FPs are generally dimmer than the highest performance synthetic dyes of similar color. The brightness of FPs spans a broad range with some commercially available proteins, such as mPlum [34] and DsRed-monomer from Clontech (Mountain View, CA), falling near or below the low end of the brightness range provided previously (Table 1.1). At the other extreme, the brightest FPs currently available are YPet at $80 \text{ mM}^{-1} \text{ cm}^{-1}$ [35] and tdTomato at $95 \text{ mM}^{-1} \text{ cm}^{-1}$ [36]. In general, the brightest FPs occur in the green, yellow, and orange color classes, whereas FPs emitting in the blue, cyan, and red spectral regions are generally dimmer. Based on the fact that a number of FPs have ECs approaching $100,000 \text{ M}^{-1} \text{ cm}^{-1}$ and the best have QYs approaching 0.8 [3], it is not unreasonable to expect that it should eventually be possible to engineer an FP color palette where each protein has a brightness of at least $80 \text{ mM}^{-1} \text{ cm}^{-1}$!

Quantitative assessment of EC and QY for an FP is relatively tedious and requires a highly purified and correctly folded protein with, ideally, greater than 95% of the molecules having an active fluorescent chromophore [37]. In addition, for EC determination the total protein concentration must be accurately determined and the measurements of absorption and fluorescence emission performed in reliable, calibrated instrumentation. QY assessment requires the comparison of emission spectra between the FP and an appropriate reference standard having a similar wavelength profile. Investigators should be highly skeptical of purely qualitative FP brightness evaluations (often made by commercial distributors) that lack quantitative information pertaining to the extinction coefficient and quantum yield. It is difficult, if not impossible, to accurately perform brightness comparisons between FPs without knowledge of these critical parameters. Further complicating matters is the fact that even if EC and QY are highly favorable, experimental brightness observed for the FP gene expressed in living cell is intrinsically dependent on the folding and maturation efficiency of the FP (discussed in the following) [37, 38].

Independent of considerations of the intrinsic brightness displayed by a particular FP, the configuration of the imaging equipment is equally and critically important to achieve high signal strength in an imaging experiment. The laser system or arc-discharge lamp coupled to fluorescence filters used to excite the chromophore should strongly overlap the chromophore absorption profile, and the emission filters must have the widest possible bandpass region coinciding with the emission spectrum. In addition, the camera system must be capable of recording images with high quantum efficiency in the fluorescence emission region of interest [39], and the optical system of the microscope should have high throughput in the wavelength regions necessary

for producing excitation and gathering emission. Even with research-level instrumentation, it is often difficult to achieve the maximum potential FP brightness levels in each spectral class unless the fluorescence filter sets are optimized for imaging the proteins. Many multiuser core imaging facilities have limited inventories of filter sets typically designed for traditional synthetic fluorophores rather than FPs. For example, the standard DAPI (4', 6-diamidino-2-phenylindole; ultraviolet excitation), FITC (fluorescein isothiocyanate; cyan-blue excitation), TRITC (tetramethylrhodamine isothiocyanate; green excitation), and Texas Red (yellow excitation) fluorescence filter combinations, often marketed by default with widefield arc-discharge microscopes, are not suitable for many FPs and are less than optimal for others.

Photostability

A commonly cited limitation of FPs relative to other fluorophore technologies is their propensity to photobleach during observation. In other words, illumination of an FP causes it to self-destruct through a series of poorly understood and likely complex mechanisms. Two probable mechanisms for photobleaching of FPs are reaction with a reactive oxygen species (ROS; i.e., singlet oxygen generated by the FP chromophore itself) and photo-induced isomerization [40]. Synthetic dyes are, of course, also susceptible to photobleaching by related mechanisms. One might expect that due to the protective protein shell that holds the FP chromophore rigid and planar and protects it from the bulk environment [41, 42], FPs should be significantly more photostable than a fluorescent dye. Generally speaking, this is not true, and for the FPs considered “best in class,” the average photostability is on par with that of the widely used synthetic dye, fluorescein [3]. The most photostable of all currently available monomeric FPs is mEGFP, which is ~ 33 -fold more photostable than fluorescein. The fluorescence of fluorescent nanoparticles (or quantum dots) does not rely on the conjugated systems of double bonds that are the “Achilles heel” of FPs and synthetic dyes with respect to photobleaching. For this reason, nanoparticles have greatly improved photostability over even the best FPs and synthetic dyes [30].

Although there is a high degree of uncorrelated variability between FPs in terms of photostability, most variants listed in Table 1.1 are useful for short-term imaging (from 1 to 25 captures), while several of the more photostable proteins can be employed in time-lapse sequences that span periods of 24 h or longer (in which hundreds to thousands of images are gathered). The long-term stability of any particular protein, however, must be investigated for every illumination scenario (widefield, confocal, multiphoton, swept-field, etc.) because nonlinear differences in photostability are often observed with the

Table 1.1. A compilation of properties of the most useful FP variants. Along with the common name and/or acronym for each FP, the peak excitation (Ex) and emission (Em) wavelengths, molar extinction coefficient (EC), quantum yield (QY), relative brightness, and physiologically relevant quaternary structure are listed (*signifies a weak dimer). The computed brightness values were derived from the product of the molar extinction coefficient and quantum yield, divided by the value for EGFP. This listing was created from scientific and commercial literature resources and is not intended to be comprehensive, but instead represents FP derivatives that have received considerable attention in the literature and may prove valuable in research efforts. The excitation and emission peak values listed may vary in published reports due to the broad spectral profiles. In actual fluorescence microscopy investigations, the experimental brightness of a particular FP may differ (in relative terms) from the brightness provided in this table. Among the many potential reasons for these differences are wavelength-dependent differences in the transmission or reflectance of microscope optics and the efficiency of the camera. Furthermore, the extent of FP folding and maturation will depend on both the particular variant being used as well as the particular characteristics and localization of the fusion partner

Protein (Acronym)	Ex (nm)	Em (nm)	EC $\times 10^{-3}$ M ⁻¹ cm ⁻¹	QY	Quaternary Structure	Relative Brightness (% of EGFP)	Reference
Blue Fluorescent Proteins							
Azurite	384	450	26.2	0.55	Monomer*	43	[91]
EBFP2	383	448	32.0	0.56	Monomer*	53	[57]
mTagBFP	399	456	52.0	0.63	Monomer	98	[100]
Cyan Fluorescent Proteins							
ECFP	439	476	32.5	0.40	Monomer*	39	[185]
TagCFP	458	480	37.0	0.57	Monomer	63	Evrogen
mCerulean	433	475	43.0	0.62	Monomer*	79	[88]
CyPet	435	477	35.0	0.51	Monomer*	53	[35]
AmCyan	458	489	44.0	0.24	Tetramer	31	[22]
Midoriishi Cyan	472	495	27.3	0.90	Dimer	73	[73]
mTFP1	462	492	64	0.85	Monomer	162	[77]
Green Fluorescent Proteins							
EGFP	488	507	56.0	0.60	Monomer*	100	[17]
Emerald	487	509	57.5	0.68	Monomer*	116	[97]
Azami Green	492	505	55.0	0.74	Monomer	121	[72]
mWasabi	493	509	70.0	0.80	Monomer	167	[107]
ZsGreen	493	505	43.0	0.91	Tetramer	117	[22]
TagGFP	482	505	58.2	0.59	Monomer	102	Evrogen
Superfolder avGFP	485	510	83.3	0.65	Monomer*	160	[55]
T-Sapphire	399	511	44.0	0.60	Monomer*	79	[44]
Yellow Fluorescent Proteins							
EYFP	514	527	83.4	0.61	Monomer*	151	[186]
Topaz	514	527	94.5	0.60	Monomer*	169	[60]
Venus	515	528	92.2	0.57	Monomer*	156	[56]
Citrine	516	529	77.0	0.76	Monomer	174	[92]
YPet	517	530	104	0.77	Monomer*	238	[35]
ZsYellow	529	539	20.2	0.42	Tetramer	25	[22]
TagYFP	508	524	64.0	0.60	Monomer	118	Evrogen
mAmetrine	406	526	45.0	0.58	Monomer	78	[187]
Orange Fluorescent Proteins							
Kusabira Orange	548	559	51.6	0.60	Monomer	92	[73]
Kusabira Orange2	551	565	63.8	0.62	Monomer	118	[114]
mOrange	548	562	71.0	0.69	Monomer	146	[36]
mOrange2	549	565	58.0	0.60	Monomer	104	[115]
dTomato	554	581	69.0	0.69	Dimer	142	[36]
dTomato-Tandem	554	581	138	0.69	Pseudo Monomer	283	[36]
DsRed	558	583	75.0	0.79	Tetramer	176	[22]
DsRed-Express (T1)	555	584	38.0	0.51	Tetramer	58	[188]
DsRed-Monomer	556	586	35.0	0.10	Monomer	10	Ciontech
TagRFP	555	584	100.0	0.48	Monomer	142	[118]
TagRFP-T	555	584	81.0	0.41	Monomer	99	[115]
Red Fluorescent Proteins							
mRuby	558	605	112.0	0.35	Monomer	117	[126]
mApple	568	592	75.0	0.49	Monomer	109	[115]
mStrawberry	574	596	90.0	0.29	Monomer	78	[36]
AsRed2	576	592	56.2	0.05	Tetramer	8	[22]
mRFP1	584	607	50.0	0.25	Monomer	37	[64]
JRed	584	610	44.0	0.20	Dimer	26	[93]
mCherry	587	610	72.0	0.22	Monomer	47	[36]
HcRed1	588	618	20.0	0.015	Dimer	1	[123]
mRaspberry	598	625	86.0	0.15	Monomer	38	[34]
mKate	588	635	45.0	0.33	Monomer	44	[128]
HcRed-Tandem	590	637	160	0.04	Pseudo Monomer	19	[78]
mPlum	590	649	41.0	0.10	Monomer	12	[34]

same protein when illumination is produced by an arc-discharge lamp versus a laser system. The molecular basis of nonlinear differences in photobleaching of FPs versus light intensity and wavelength is largely an open question that we hope will be addressed in the future. In terms of photostability, the selection of a suitable FP is dictated by numerous parameters, including the illumination conditions, the expression system, and the effectiveness of the imaging setup.

Color Class

What does “color” mean in the context of fluorescence? It could, reasonably, refer to the perceived color of a solution of the fluorophore when viewed in white light. The term could also, reasonably, refer to the perceived color of the solution when illuminated with monochromatic light of a wavelength that corresponds to the absorbance maxima. In practice, any attempt to define fluorescence color by virtue of how it is perceived by eye leads to complications. A more rigorous and practical approach to defining fluorescence color is to say that two fluorophores have different color if their excitation and/or emission maxima and/or peak shapes are significantly different. Defining “significantly different” is troublesome as it depends on the instrumentation available for measuring the shape and maxima of the emission and excitation peaks. For example, spectral imaging can be used to differentiate two colors that could not be differentiated through the use of bandpass filters.

Regardless of whether one considers synthetic fluorophores, FPs, or quantum dots and assuming all other considerations are the same, how will the researcher choose which color to use? An important consideration with respect to color selection is the greater desirability of red-shifted fluorophores [43]. It is generally accepted that excitation with violet or blue light is associated with greater cellular phototoxicity than excitation with green, yellow, or longer wavelength light extending through the near infrared (up to ~1000 nm) but not into the true infrared (where heating due to absorption by water would be problematic for cell viability). Fluorescence excitation and emission hues of FPs are confined to a relatively narrow region of the electromagnetic spectrum (essentially the visible wavelengths) due to protein-imposed restrictions on the possible manipulations of the chromophore structure and environment. In contrast, synthetic dyes and nanoparticles with fluorescence emission tuned to wavelengths that cover the visible and near-infrared regions of the spectrum are available. This spectral limitation of FPs is exacerbated by their relatively broad excitation and emission peaks (ranging up to 100 nm) that further restrict the number of colors that can be distinguished with bandpass filters on a widefield microscope. Practically speaking, the bandwidth of the absorption and emission peaks is

an important consideration in defining the number of colors that are “spectrally distinct.” Roughly speaking, there are currently about ten different emission colors of FPs with short Stoke shifts (defined as the distance in nanometers between the absorption and emission peak wavelengths of a fluorophore) and emission maxima spaced every 20 nm between 450 and 650 nm (Table 1.1). These colors include: blue (~450 nm), cyan (~470 nm), teal (~490 nm), green (~510 nm), yellow (~530 nm), yellow–orange (~550 nm), orange (~570 nm), orange–red (~590 nm), red (~610 nm), and far-red (>630 nm). There are a few additional long Stoke shift FPs such as Sapphire [44] and mKeima [45], which, given the definition of fluorescence color provided previously, should be considered additional color classes. However, due to the relatively broad excitation and emission peaks shared by all FPs, it is only really practical to simultaneously image three (Figure 1.3 [46]) or four distinct colors (such as cyan, yellow, and red or blue, green, orange, and far-red) using a bandpass filter-based microscopy system [3]. However, this tenet does not always hold true as the imaging of six distinct colors (CFP, cyan; mMiCy, teal; EGFP, green; YFP, yellow; dKeima570, orange; and mKeima, red) has been achieved using a single laser line for excitation and spectral unmixing of the emission [45].

Hybrid Approaches

This discussion has established that, relative to synthetic dyes and quantum dots, the physical properties of FPs are less than ideal yet more than adequate. Investigators that simply require a fluorophore with high fluorescent brightness, good photostability, and broad color selection would do better with synthetic dyes or quantum dots. However, as mentioned earlier, such superficial comparisons are a disservice to FPs because the fact that these probes are proteins, and are therefore genetically encodable, is their overwhelming advantage for many biological applications. In recent years there has been significant progress in developing “hybrid” technologies for the protein-specific labeling of recombinant proteins in live cells [47–49]. These approaches typically exploit modified dyes (or quantum dots [50]) for noncovalent binding or covalent attachment to a genetically encoded sequence that can be appended to a recombinant protein of interest. Notable examples of such methods include biarsenical xanthene dye-based labeling of tetracysteine motifs [51] and benzylguanine-dye conjugate-based labeling of O6-alkylguanine-DNA alkyltransferase fusion proteins [52], though a number of additional new systems have been reported [47–49]. Although these techniques hold great promise, none of them has yet achieved the versatility and widespread acceptance of FP-based labeling. A major limitation shared by all hybrid methodologies is the nonspecific labeling of intracellular structures with the exogenously applied dye [53]. In

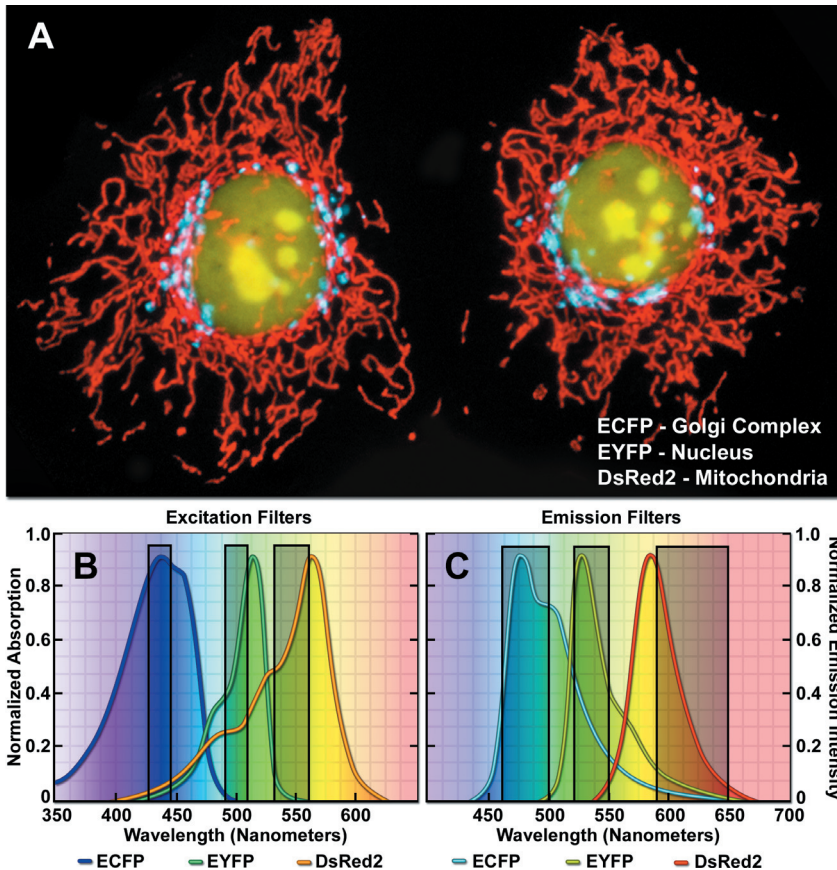


Figure 1.3. Optimized fluorescence filter combinations for multicolor imaging of three FPs spanning the cyan to orange-red wavelength regions; **(A)** Widefield fluorescence image of HeLa cells labeled with ECFP (Golgi complex targeting signal), EYFP (nuclear targeting signal), and DsRed2 (mitochondrial targeting signal); **(B)** Excitation filters optimized for ECFP, EYFP, and DsRed2 FPs having center wavelengths of 436, 500, and 545 nm, respectively. The bandwidth of the ECFP and EYFP excitation filters is 20 nm whereas the bandwidth of the DsRed2 filter is 30 nm; **(C)** Emission filters optimized for the same probes having center wavelengths of 480, 535, and 620 nm with bandwidths of 40, 30, and 60 nm, respectively.

many cases, high levels of nonspecific background staining hampers observation of the targeted structures, and several of the synthetic dyes are sequestered in the mitochondria, lysosomes, and other organelles.

DIRECT COMPARISONS OF FLUORESCENT PROTEINS TO EACH OTHER

For direct comparison of one FP to another, the properties of brightness, photostability, and color remain the three most important criteria. However, there are additional concerns that are direct consequences of the unique experimental designs made possible with FPs. For example, because these probes are proteins, they must undergo efficient transcription, translation, and folding to be functional. Once correctly folded, they then undergo autocatalytic posttranslational chromophore formation, a process informally referred to as

“maturation” or “ripening.” If the efficiency of any of these steps is compromised, the experimentally observed fluorescence will be diminished or even abolished. Such concerns are not relevant to alternative technologies such as synthetic dyes and quantum dots applied directly to the cells or tissue. In the following sections we list several of the most important criteria that can be used to directly compare FPs and discuss efforts to engineer new variants that are superior by these criteria.

Folding and Maturation Efficiency

Aequorea jellyfish inhabit the cool ocean waters off the coast of Washington and British Columbia. Accordingly, the natural environment of the avGFP protein is one where the temperature hovers around 4–5°C. In contrast, in the unnatural environment (from the FP’s perspective) of a transfected cell culture or the cells of a transgenic organism, the avGFP protein will most

often experience much higher temperatures than those in which it was evolved to fold, mature, and function. FPs derived from reef corals and sea anemones generally express well at 37° C without genetic selection, presumably because the native species from which the proteins are obtained have evolved in somewhat warmer habitats [54]. The original transposition of wild-type avGFP from jellyfish to cells grown at 37° C substantially decreased the efficiency with which the protein could fold into its proper three-dimensional (tertiary) structure. Clearly this problem needed to be addressed through protein engineering. Indeed, among the first and most substantial improvements to the avGFP protein were realized by selection of variants with more efficient folding at 37° C. Years of progress in this regard have most recently led to a so-called superfolder avGFP with improved folding kinetics, tolerance to circular permutations, high performance in fusions to poorly folding polypeptides, and resistance to denaturation [55]. One of the more interesting and useful aspects of mutations that improve folding efficiency is that they are often translated to different FP colors where they seem to provide similar improvements. The translation of so-called folding mutations to hue-shifted variants has contributed to the excellent folding properties or high brightness of the Venus YFP variant [56], EBFP2 [57], and the series of “super” cyan and yellow FPs [58, 59], among others [55].

The presence of molecular oxygen is also a critical factor in FP chromophore development during the maturation process. During the formation of chromophores in *Aequorea* protein variants, at least one oxygen molecule is required for an oxidation reaction [60, 61], whereas reef coral proteins that emit in the orange–red spectral regions usually require two molecules [62, 63]. In mammalian cell cultures, FP maturation is rarely hampered by a lack of oxygen, but anoxia could become a limiting factor in other systems.

Oligomerization

All of the FPs discovered to date display at least a limited degree of quaternary structure (self-association of individual protein units), exemplified by the weak tendency of native avGFP and its derivatives to dimerize when immobilized at high concentrations [64, 65], as well as the obligate tetrameric structure characteristic of FPs from reef coral and anemones [66, 67]. Oligomerization can be a significant problem for many applications in cell biology, particularly in cases where the FP is fused to a host protein targeted at a specific subcellular location. Once expressed, the formation of dimers and higher-order oligomers induced by the FP portion of the chimera can produce atypical localization, disrupt normal function, interfere with signaling cascades, or restrict the fusion product to aggregation within a specific organelle or the cytoplasm. This effect is particularly

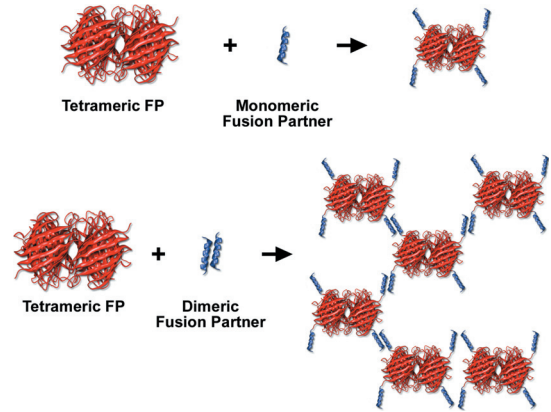


Figure 1.4. Any protein fused to a tetrameric FP will become tetrameric itself.

marked when the FP is fused to partners that participate in natural oligomer formation themselves (see Figure 1.4). Fusion products with proteins that form only weak dimers (i.e., most *Aequorea* variants) may not exhibit aggregation or improper targeting, provided the localized concentration remains low. However, when FPs are targeted to specific cellular compartments, such as the plasma membrane, the localized protein concentration can, in some circumstances, become high enough to permit dimerization.

The basic strategy for overcoming oligomerization artifacts is to modify the FP amino acid sequence to include residues that disrupt intermolecular interactions, a procedure that varies in complexity depending upon the nature and origin of the protein. For many avGFP variants, dimerization can be either significantly reduced or eliminated by replacing the hydrophobic amino acid side chains in the dimer interface with positively charged residues at several key sequence positions [65]. The three most successful mutations, in decreasing order of effectiveness, are A206K, L221K, and F223R, where the non-polar amino acids alanine, leucine, and phenylalanine are replaced by one of the positively charged hydrophilic amino acids lysine or arginine. In cases where close molecular associations are suspected involving a fusion protein and where quantitative FRET interactions are investigated, it is highly recommended that avGFP variants (i.e., CFP and YFP) be converted into monomers using the A206K point mutation [3, 68].

Creating FP monomers from the tetrameric reef coral and sea anemone proteins is usually far more difficult. Even at exceedingly low concentrations, the original DsRed FP is an obligate tetramer [66] that cannot be dissociated without irreversible denaturation of the polypeptides. In the tetrameric unit, each DsRed protomer interacts with two adjacent neighbors, one through a hydrophobic interface and the other through a hydrophilic interface resulting in a complex assembly

[69, 70]. Other Anthozoa proteins, such as the *Zoanthus* variants and eqFP611, apparently have weaker interactions between the units of the tetramer and may be easier to disrupt into monomers [71]. The most successful approaches [64, 68] have involved the use of site-directed mutagenesis to disrupt the tetrameric interfaces, usually by substitution of hydrophilic or charged amino acids for hydrophobic and neutral moieties. Following the precedent of the process used to break DsRed into a monomeric variant [64], a growing number of coral-derived FPs have now been monomerized. Some notable examples include a green FP from *Galaxeidae* [72]; an orange FP from the *Fungia concinna* [73]; photoconvertible FPs from both *Lobophyllia hemprichii* [74] and *Dendronephthya* [75]; a photoactivatable GFP from *Pectiniidae* [76]; a chromoprotein from *Montipora* [45]; and a cyan FP from *Clavularia* [77].

Another useful technique for preventing oligomerization artifacts for dimeric fluorescent proteins involves creating vectors containing two sequential coding regions separated by a short unstructured linker. Upon expression, the fused FPs, known as “tandem dimers,” preferentially bind to each other to form an intramolecular dimeric unit that performs essentially as a monomer although at twice the molecular weight (and size). Tandem dimer constructs have been developed with DsRed derivatives [36, 64], HcRed [78], and a photoconvertible FP known as EosFP [79]. A somewhat different strategy for reducing or eliminating the artifacts associated with FP oligomerization is to simultaneously coexpress FP-tagged proteins with an excess of a nonfluorescent mutant of the same FP [80, 81]. Related to the problem of FP oligomerization is the problem of FP aggregation. Although oligomerization tends to refer to the ability of some FPs to form well-defined quaternary structures, aggregation refers to the tendency of some FPs to act somewhat sticky toward themselves and to form poorly defined complexes of indeterminate stoichiometry. The problem of aggregation seems to be confined to coral-derived FPs and is not generally recognized as a problem with *Aequorea*-derived FPs. An effective strategy for minimizing FP aggregation is the removal of several basic residues that seem to be primarily responsible for the tendency to aggregate from the N-terminus of the FP [82]. Regardless of the specific mechanism employed to overcome FP oligomerization and/or aggregation, the most important point is that experimental results are not compromised by artifacts induced by the existence of quaternary structures.

Although it is generally agreed that a monomeric FP is more desirable than an oligomeric FP, there is at least one case where an oligomeric structure can be advantageous. Dimerization of a FRET pair containing FPs can result in particularly efficient FRET if the chromophores are appropriately oriented. High levels of FRET are desirable in the case of FRET-based sensors of protease activity

(e.g., caspase sensors) because cleavage of the substrate (the inter-FP linker) causes dissociation of the FPs and loss of FRET. The higher the FRET level in the initial construct, the greater the change in signal once the linker has been digested. For example, evolutionary optimization of a caspase-3 sensor based on CFP and YFP produced a new FRET pair, known as CyPet and YPet, with greatly improved FRET efficiency [35]. The improved FRET efficiency in the intact state necessarily leads to a substantially improved ratiometric change upon linker cleavage. However, subsequent work has revealed that CyPet and YPet actually have an increased tendency to dimerize in an as yet undetermined orientation compatible with high FRET efficiency [83, 84].

Fusion Tolerance

The most common application for FPs is in the creation of a functional chimera (or fusion) with a second, target protein that is of particular interest to a researcher. In the ideal situation, the appended FP would have no effect on the normal folding, localization, biological function, and molecular interactions of the fusion partner. Similarly, the host would ideally have no adverse effect on the folding and maturation of the FP. This requirement poses an important question: In what percentage of fusion proteins are both the FP and the host protein well behaved? Unfortunately, there is no definitive answer. Although the literature is loaded with examples of successful fusions, it is likely that many unsuccessful fusions are never published. In addition, it is possible that in many cases the success or failure of a particular chimera depends on specific details, such as whether it was an N- or C-terminal fusion, the linker length, and the particular identity of the FP. For lack of a better mechanism for addressing this question, we can turn to a study in which avGFP fusions were created with every open reading frame (ORF) of the budding yeast, *Saccharomyces cerevisiae*. Of the 6234 ORFs investigated, 4154 (or 67%) resulted in expression of green fluorescence [85]. Although it is not clear exactly what fraction of these fusions retained full functionality of the host protein, it is also unknown how many of the 33% additional ORFs may have yielded to an alternate fusion topology, linker, or FP variant. With these caveats in mind, two-thirds is probably a reasonably conservative approximation of the fraction of FP fusions that will be well behaved. Multimodality fusion reporter genes are further discussed in Chapter 5.

Fluorescence Lifetime Properties

Although the issues described previously are pertinent to virtually all researchers who employ FPs, the homogeneity of the lifetime decay is of importance to only the growing subset of investigators who employ FPs for fluorescence lifetime imaging microscopy (FLIM) [86].

Whereas standard fluorescence microscopy detects the spatially and wavelength-resolved fluorescence intensity of FPs in cells, FLIM detects the spatially and wavelength-resolved decay of the nanosecond-scale excited state for fluorophores. Thus, in FLIM experiments the nanosecond decay kinetics of the FP chromophore electronic excited state (referred to as the fluorescence lifetime, τ) is determined in spatial coordinates using a specialized microscope detector capable of high-frequency modulation or fast gating.

This approach offers certain advantages over intensity-based methods for cellular imaging, such as being independent of fluorophore concentration and having an exquisite sensitivity toward the chromophore environment. FLIM is particularly useful in combination with FRET for difficult measurements that are not conducive to acceptor photobleaching or sensitized emission methods. However, the very sensitivity that makes FLIM a useful technique also presents additional complexities and technical challenges for data acquisition. The most relevant issue is that many FPs display complex multiple-lifetime decays. Interpretation of FLIM data is therefore nontrivial due to the fact that these decay modes are made even more complex by the heterogeneity of the intracellular environment and the presence of FRET acceptors [87]. This issue could be addressed by development of new FP FRET pairs in which the donor has a homogeneous lifetime decay, and such a goal is widely recognized in FP engineering [77, 88]. Unfortunately, fluorescence lifetime is a good example of a property that is difficult to select in the type of screens typically used in directed evolution of new FPs.

Does Newer Always Mean Better?

With the ever-growing number of new FP variants and the ongoing reengineering of various generations of individual FPs, picking the “best” FP for a particular application is becoming increasingly more confusing. As a general rule of thumb we recommend sticking with those FP variants that are “tried-and-true” rather than simply choosing the most recently published variant. Numerous factors have the potential to negatively impact the performance of an FP in a particular experiment, and new FP variants rarely see testing against all these factors prior to publication. For example, although a new FP variant may behave well in the few standard test fusions attempted by the developers, it might not be practical for all conceivable protein fusions. Even weak residual dimerization for a protein engineered to be monomeric could perturb the localization of some fusions (but not others). Additional subtle factors include the fact that certain FPs are “stickier” (more prone to aggregation) than others and may, under certain conditions, mislocalize due to nonspecific interactions between charged or hydrophobic patches on the surface of the protein. The ultimate validation for an

FP is, of course, widespread critical evaluation followed by eventual acceptance by the research community. Using this strictest of criteria, the one FP that stands above the crowd is the avGFP-derived EGFP variant, which exhibits good to excellent performance by all criteria listed previously. Another particularly well-validated and robust FP is the DsRed-derived mCherry, which is an excellent choice for a second color to pair with EGFP.

ENGINEERING IMPROVED FLUORESCENT PROTEINS

As a class, FPs have been subjected to more extensive protein engineering and artificial directed evolution than almost any other class of protein. Why have FPs received so much attention in this regard? The simple answer is that FPs are extremely popular tools in the biological sciences and improved variants can provide huge benefits to researchers. However, this is not the entire story, and there are two additional factors at play. The first factor is that often the very same researchers who employ FPs in their research are the ones who recognize the deficiencies and have the skills to address them. Specifically, researchers who employ FPs are typically experts in molecular biology and fluorescence spectroscopy and microscopy; exactly the tools necessary to undertake engineering of FPs for improved properties. Contrast this to the example of a cell biologist who is dissatisfied with the pharmacological specificity of a particular kinase inhibitor. The cell biologist will almost certainly lack the skills and resources necessary to undertake the synthesis of a potentially more specific inhibitor. The second factor is that, by the very nature of the property that makes them useful tools (i.e., their intrinsic visible fluorescence), identification of FP variants with, for example, improved brightness or a substantial color shift is relatively straightforward.

Fluorescent Protein Engineering and Directed Evolution: General Principles

The defining feature of avGFP is its remarkable ability to autonomously generate a fluorophore within the confines of its distinctive β -barrel structure (see Figure 1.5) [41, 42, 89]. The steric, electrostatic, and hydrogen-bonding environment imposed upon the chromophore by the surrounding residues strongly influences the fluorescence properties. Remarkably and perhaps fortunately, the avGFP chromophore was found to be highly amenable to genetic modification of both its covalent structure and localized environment, and this tolerance has been exploited for the creation of wavelength-shifted variants [60] spanning an 80-nm range. In addition, the avGFP protein is also very tolerant of modifications of residues with side chains that are

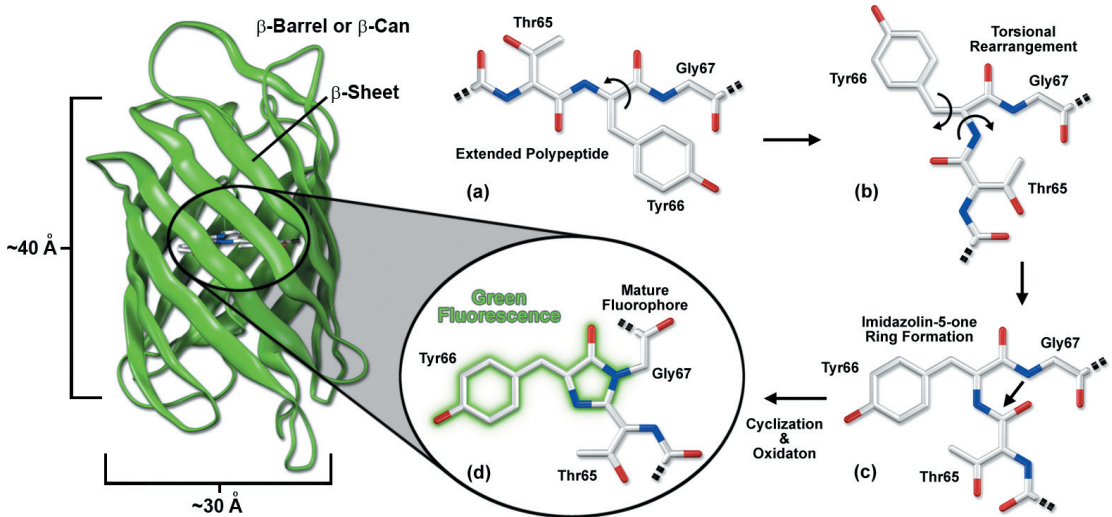


Figure 1.5. Schematic diagram of the β -barrel structure and chromophore formation in maturing enhanced green fluorescent protein (EGFP). (A) The prematuration EGFP fluorophore tripeptide amino acid sequence (Thr65-Tyr66-Gly67) is stretched into a linear configuration so that the threonine residue is positioned in the upper left-hand corner of the diagram. The first step in maturation is a series of torsional adjustments (B) and (C) that relocate the carboxyl carbon of Thr65 so that it is in close proximity to the amino nitrogen of Gly67. The nucleophilic attack of the amide nitrogen of Gly67 on the carboxyl group of Thr65 (C), followed by dehydration, results in formation of an imidazolin-5-one heterocyclic ring system. (D) Fluorescence occurs when oxidation of the tyrosine α - β carbon bond by molecular oxygen extends electron conjugation of the imidazolin-5-one ring system to include the tyrosine residue.

external to the β -barrel, including those on the surface of the barrel and additions (along with limited truncation) at the N- and C-termini of the protein. Efforts to genetically modify the structure of FPs can be broadly classified into two categories: rational modifications and irrational modifications. The former category would contain all FP fusion proteins that are obviously rationally designed and constructed to address a specific biological question. However, when it comes to efforts to modify the FP itself for the purposes of engineering new colors or otherwise improved variants, irrational approaches tend to be more effective than rational approaches.

Generally speaking, our ability to make rational modification of any protein (FPs included) to generate variants with new properties is sadly limited. Accordingly, the number of successful avGFP modifications that probably seemed rational *a priori*, and were ultimately experimentally validated, are relatively few in number. Some important examples of rational mutations of avGFP include Tyr66Trp to create CFP and its descendents [18]; Tyr66His to create BFP and its descendents [18]; introduction of a stacking residue at residue Thr203Tyr to create YFP and its progeny [42]; and the monomerizing mutation Ala206Lys [65] (Figure 1.6). Each of these

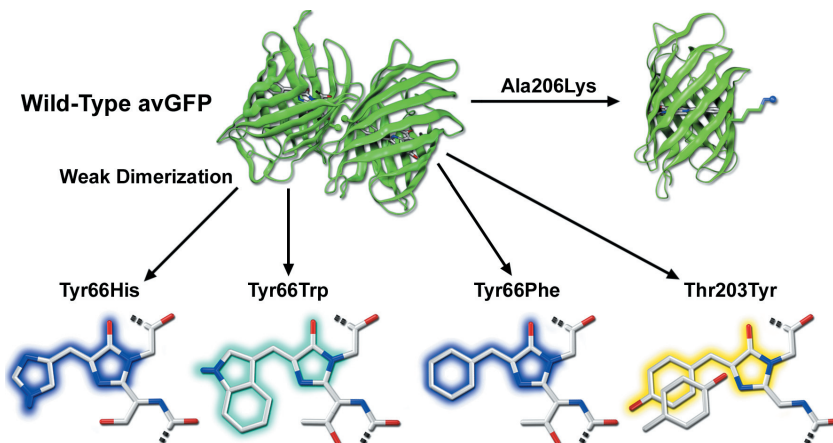


Figure 1.6. Rational modifications of avGFP.

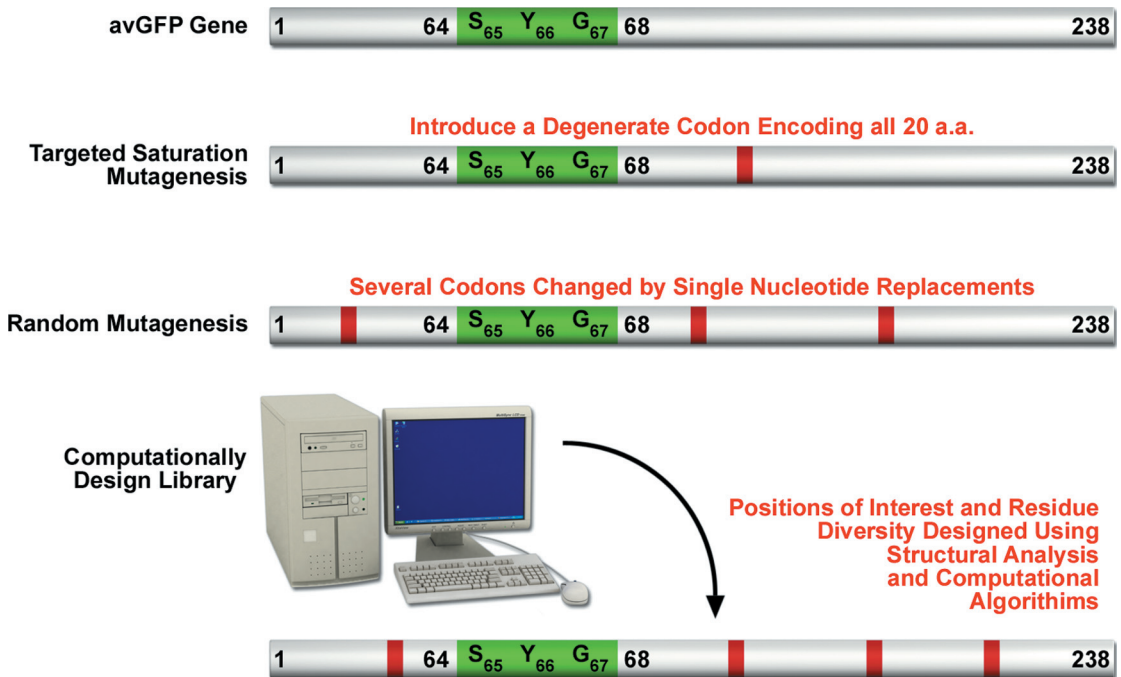


Figure 1.7. Strategies for creation of libraries of FP variants.

modifications involves dramatic changes in the chromophore structure, the chromophore environment, or the nature of oligomeric interactions. Rational modifications of proteins are almost never subtle! However, these dramatic changes are often the critical first steps that ultimately lead to the development of important variants with new colors or properties. From the perspective of protein evolution, rational modifications tend to represent artificially induced evolutionary leaps that stand in marked contrast to the baby-steps that would tend to characterize protein evolution in the wild. Unfortunately, these rational changes are almost always accompanied by substantially decreased fluorescent brightness. To “rescue” the fluorescent brightness of a new variant requires the introduction of compensating mutations compatible with the original rational modification. This is where irrational approaches are most effective. For example, during the breakup of tetrameric DsRed into a functional monomer, the initial mutagenesis efforts designed to disrupt oligomerization resulted in a dramatic reduction in red fluorescence. Subsequent rounds of targeted and random mutagenesis successfully directed the evolution of DsRed into a bright monomer in eight generations.

As they are defined here, irrational approaches attempt to mimic the process of natural protein evolution. That is, the gradual accumulation of mutations that each confer a small, but additive, benefit. These modifications tend to be subtle “tweaks” of the protein structure (far too subtle to be rationally designed), often

involving slight shifts in the packing of hydrophobic cores or in the placement of buried hydrogen bond donors and acceptors or electrostatic charges. Our understanding of protein structure and function is inadequate for rational prediction of which particular mutations might be beneficial. Fortunately, the subtlety and effectiveness of natural protein evolution can be effectively mimicked and even greatly accelerated in the research laboratory. In laboratory-based directed protein evolution, genetic diversity is created through the use of molecular biology (Figure 1.7), and then the resulting library of protein variants is screened to identify variants with improved properties. The primary advantage of this approach is that it does not require a complete understanding of the protein structure and function to be successful. Indeed, it is often difficult to rationalize beneficial mutations identified through this approach.

The key to success for directed evolution of proteins is having an effective high-throughput screen to identify mutant proteins with favorable properties. It should be noted that only those properties being screened for will be caught in the assay, whereas those not being monitored, either beneficial or deleterious, will pass through unnoticed. With respect to directed evolution of FPs, the easiest screen to perform is based on the brightness of the FP when expressed in bacteria. Accordingly, this approach can produce FPs that are brightly fluorescent, but in some cases only when expressed in bacteria. The same variant may or may not be as brightly fluorescent when expressed in other cell types or when expressed as

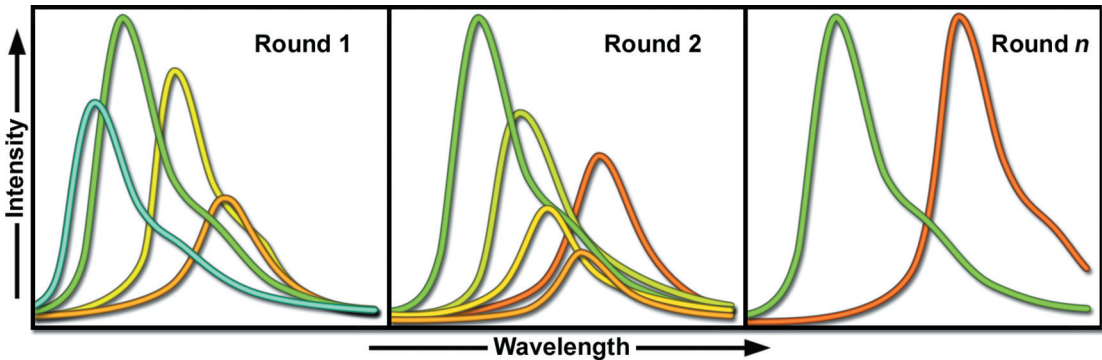


Figure 1.8. Hypothetical representation of the directed evolution of a red-shifted FP.

a fusion to another protein. Consistent with this corollary, FPs evolved only for brightness have not been subjected to selective pressure for photostability, color, or the homogeneity of the lifetime decay, and thus will most likely not be optimal with respect to these important properties. A major challenge for the future is designing library screens that will simultaneously select for variants improved by all relevant criteria. As yet, there has been scant progress in this area beyond the simultaneous screening for brightness and photostability [4].

Figure 1.8 shows a hypothetical series of emission profiles for FPs identified during the process of directed evolution for a new property; in this case a red-shifted emission peak. The intention of this figure is to illustrate general principles of how laboratory evolution of an FP tends to proceed. The green line is the fluorescent emission profile of the progenitor FP. The gene encoding this progenitor FP has undergone diversification by any of a number of strategies (Figure 1.7). In the first round of library screening, a variety of variants with shifted emission maxima, but dimmer fluorescence, were identified. In general, more dramatic color changes (spectral shifts of fluorescence emission) produce more substantial adverse effects on fluorescent brightness. The most red-shifted variant in Figure 1.8 (orange line) was chosen as the template for library creation in the second round. Library screening resulted in the identification of variants with incrementally improved brightness and minor shifts in emission maxima. To be successful, the researcher must choose the variant that is the best compromise of brightness and red shift to carry into the next round of evolution. Fluorescence-activated cell sorting (FACS) is often a method of choice for screening of FP libraries because it enables the rapid screening of millions of variants and with rapid isolation of only the brightest cells [34–36, 90, 91]. Repeating this process through many rounds will often (but not always) result in a new FP color with brightness that equals or exceeds the original protein. For example, Citrine [92] and Venus [56] are red-shifted variants derived from EGFP yet exceed their parent in brightness. It has been demonstrated on

numerous occasions that extensive directed evolution can produce new colors of FP with exceptional brightness. Recent examples include the development of the brightest cyan (or teal) [77] and blue [57] FPs currently available. On the other hand, extensive selection for red-shifted variants was ultimately successful in producing mPlum, which is red-shifted in its emission by 42 nm but only a third as bright as its progenitor, mRFP1 [34].

The Future of Fluorescent Protein Engineering

Through a combination of rational and random mutagenesis, the properties of the most useful FP variants have continued to improve incrementally. With such widespread adoption, one might think of the FPs as mature, optimized tools. However, this is not the case, and the biochemical and photophysical properties of FPs still limit their utility in many applications. It is interesting to note that most FP development to date has focused on just two parent genes: that of the avGFP and the *Discosoma* RFP. The known FPs obtained from phylum Cnidaria are now more than one hundred, and this quantity promises to keep growing [24]. FPs have recently been cloned from organisms of the phylum Arthropoda [25, 93], so protein engineers may soon have access to a new selection of templates from which to evolve exciting new variants.

An obvious direction for future work in developing improved FPs is the engineering of new variants with improved photostability. However, it may not be immediately obvious how one might go about screening FP libraries to identify variants with improved photostability. This is certainly a much more difficult property to screen for than simple fluorescent brightness. One approach proven to be effective in identifying variants with improved photostability is bleaching of FP libraries with an array of intense light emitting diodes (LEDs) [77]. Repeated rounds of selection for variants that bleached the slowest when exposed to intense blue light from an LED array eventually resulted in the

identification of mTFP1 (teal FP), which was more than 100-fold more photostable than its progenitor, mTFP0.7. It is possible that applying similar approaches to other FPs could provide similar improvements in photostability. Another approach proven successful is the use of FACS [91], which successfully enriched a highly photostable variant of EBFP from a large library of variants, simply by selecting for the brightest variants. In this case, bleaching during the brief passage of single cells through the intense excitation laser beam may have been significant enough to decrease the overall intensity for the least photostable members of the library. Alternatively, ROS generated during extensive photobleaching may have been toxic to those cells harboring the least photostable members of the library. Despite these few promising examples, it is clear that if dramatic improvements in photostability are to be realized for the most photostable of the FPs (i.e., beyond their already good photostability), much longer exposures and/or much more intense light sources will be required for the FP library bleaching screens.

Other important goals for protein engineers include the development of brighter and more red-shifted RFP variants; ideally with emission extending into the so-called near-infrared window where tissue absorbance is at minimum [43]. Yet another objective will be the development of FPs with homogeneous fluorescence lifetimes. To address these goals, we expect that the design and screening of FP libraries will become more sophisticated as computational methods and multiparameter high-throughput screens become the norm. As more diverse FP sequences are deposited in the nucleotide databases, it is likely that researchers will embrace the creation of fully synthetic FP libraries guided by sequence alignments and consensus FP sequences [94]. Eventually we can expect *de novo* computationally designed libraries [95] in which the excited state dynamics and electronic structure of the chromophore are taken into consideration.

A recurring theme in FP engineering is that there is no one candidate best suited for all applications. Most likely this trend will hold true for the future and when (or if) we eventually do manage to develop FPs that are super-bright, super-photostable, and super-red shifted by today's standards, they will all be separate proteins of diverse origin. That is, no one protein will ever combine the best of all properties, and choosing the right FP for the experiment at hand will necessarily require a compromise with respect to some other property. We are optimistic that these compromises will be fairly minor relative to the benefits. Although an impressive degree of progress in FP development has been made to date, the temptation to say that the current FP palette is "good enough" should be actively resisted. In most cases, current FP variants are good enough to meet the demands of many current applications; in all probability these proteins will not perform as needed in future applications.

THE FLUORESCENT PROTEIN COLOR PALETTE

Over the past decade, a wide variety of new FP variants have been developed featuring fluorescence emission profiles spanning a 200-nm region of the visible light spectrum (~ 450 nm to ~ 650 nm), providing useful genetically encoded fluorophores in essentially every color class (Table 1.1) [1, 3, 67]. The fundamental origins of FP emission color have been established and are generally governed by the physical extent of π -orbital conjugation contained within the chromophore [96]. This factor largely determines the general spectral class (i.e., blue, cyan, green, yellow, or red), which can involve a change in the absorption and emission maxima by hundreds of nanometers. Smaller variations in the absorption and emission maxima (ranging from 20 to 40 nm) can be attributed, as discussed previously, to local environmental variables that include the position of charged amino acid residues, hydrogen bonding networks, and hydrophobic interactions within the local chromophore environment. Continued investigations into the photophysics of the FP chromophore will no doubt yield further clues concerning the structure–function relationship with the polypeptide backbone and amino acid side chains, thus rendering the task of engineering more finely tuned color variants and broadening the spectral range much easier.

Blue and Cyan Fluorescent Proteins

Recent advances in developing new FPs in the blue and cyan spectral regions have strengthened the potential for multicolor imaging using proteins that emit in shorter wavelengths. FPs emitting in the blue region (ranging from ~ 440 nm to 470 nm) were first obtained from site-directed mutagenesis efforts targeted at the tyrosine amino acid residue at position 66 in the avGFP chromophore. Conversion of this residue to histidine (Y66H) produces a blue FP (BFP) that exhibits a broad absorption band in the ultraviolet centered close to 380 nm and an emission maximum at 448 nm [18, 97]. The original protein exhibited only about 15% to 20% of the parent avGFP brightness value due to a low quantum yield and required additional secondary mutations to increase its folding efficiency and expression levels. Subsequent investigations and several additional mutations led to an enhanced BFP version (EBFP) that was still only 25% as bright as EGFP [19] and displayed poor photostability compared to many other FPs.

Caution should be exercised when imaging live cells expressing any of the blue FPs. Aside from limited brightness levels and rapid photobleaching (compared to other FPs), blue FPs also suffer from the fact that they must be excited with ultraviolet light, which is highly phototoxic to mammalian cells, even in limited doses [98,

99]. Furthermore, inherent cellular autofluorescence and high absorption levels by cells and tissues, as well as light-scattering artifacts, often hamper imaging with excitation light in this spectral region. Microscopes operating in the ultraviolet also require specialized light sources, optics, and filter combinations that further complicate imaging. For all of these reasons, the quest for more efficient blue FPs has only recently been renewed.

Using a combination of structurally targeted libraries coupled to random and site-directed mutagenesis, three protein engineering groups have recently reported improved blue *Aequorea* FP variants that feature significantly higher brightness and photostability compared to EBFP [57, 59, 91]. Named Azurite, SBFP2 (strongly enhanced blue FP), and EBFP2, these proteins offer the first real hope for successful long-term imaging of live cells in the blue spectral region (see Table 1.1). The brightest and most photostable of the new blue *Aequorea* FPs, EBFP2 (Figure 1.1a), exhibits typical avGFP-like behavior in fusions and is an excellent FRET donor for proteins in the green spectral class [4]. Recently, an orange-emitting FP derived from coral termed TagRFP (discussed in the following) was subjected to a combination of site-directed and random mutagenesis to produce a blue variant named mTagBFP [100], which exhibits greater brightness and photostability than any previously reported blue FP. The utility of mTagBFP in fusions is similar to other coral-derived FPs (M. W. Davidson, unpublished), and this variant may well emerge as one of the most useful probes in this class. All of the blue FPs can be readily imaged in a fluorescence microscope using standard DAPI filter sets or proprietary BFP sets available from aftermarket optical filter manufacturers.

FPs in the cyan spectral region (~470 nm to 500 nm) have been widely applied as FRET donors when paired with yellow-emitting FPs [101]. This spectral class was dominated by variants of the original *Aequorea* ECFP until the introduction of a monomeric teal-colored FP, known as mTFP1 [77, 102]. Teal FP exhibits higher brightness and acid stability compared to *Aequorea* CFPs and is far more photostable. Derived from a synthetic gene library built around a *Clavularia* soft coral tetrameric protein, mTFP1 (Figure 1.1d) displays slightly red-shifted spectral characteristics compared to most cyan proteins. In general, members of the cyan FP class contain the amino acid tryptophan at position 66 in the chromophore, but mTFP1 contains the classical tyrosine residue at this location. This amino acid substitution reduces the broad fluorescence emission spectral bandwidth from approximately 60 nm to 30 nm, which is useful in reducing bleed-through in multicolor experiments. The high-emission quantum yield (see Table 1.1) of mTFP1 provides an excellent alternative to the cyan derivatives, such as ECFP [20] and Cerulean (Figure 1.1c; [88, 103]), as a FRET donor when combined with either yellow or orange FPs. For optimal imaging, mTFP1

requires a specialized filter set, but this fluorophore can still produce suitable signal levels with a standard ECFP set. However, mTFP1 is not useful for dual imaging with EGFP due to excessive bleed-through of the teal protein into the green emission channel.

Continued investigation has produced additional useful FPs in the cyan spectral class. Among the improved cyan FPs recently introduced, CyPet [35] and the enhanced cyan variant termed Cerulean [88] show the most promise for use as fusion tags, donors in FRET biosensors, and multicolor imaging. The Cerulean fluorescent probe (named for the sky-blue color) was engineered by site-directed mutagenesis of ECFP (Figure 1.1b) to yield a higher extinction coefficient, improved quantum yield, and a fluorescence lifetime decay having a single exponential component. Cerulean is at least two-fold brighter than ECFP and has been demonstrated to significantly increase contrast as well as the signal-to-noise ratio when coupled with yellow-emitting FPs, such as Venus (see the following), in FRET investigations. The abundance of advantageous features afforded by Cerulean render this protein the most useful all-purpose cyan derivative.

The CFP variant named CyPet (cyan FP for energy transfer) was derived through a unique strategy utilizing FACS to optimize the cyan and yellow pairing for FRET [35]. Libraries were screened for FRET efficiency and the best clones were subjected to several evolutionary cycles consisting of random mutagenesis and synthetic DNA shuffling. A total of seven mutations were accumulated during the directed evolution of the CyPet protein, which features absorption and emission maxima positioned at 435 nm and 477 nm, respectively. CyPet is about half as bright as EGFP and two-thirds as bright as Cerulean, but expresses relatively poorly at 37° C [3]. However, CyPet has a more blue-shifted and narrower fluorescence emission peak than CFP, which greatly increases its potential usefulness for multicolor imaging applications.

The introduction of beneficial “folding” mutations into monomeric variants of ECFP has resulted in the production of new variants featuring enhanced brightness, folding efficiency, solubility, and FRET performance [104]. Termed “super” CFPs (SCFPs), the engineered variants are significantly brighter than the parent protein when expressed in bacteria and almost twofold brighter in mammalian cells. The authors speculate that these high-performance FPs should be useful for fusion tags and in creating new CFP-YFP FRET biosensors exhibiting high dynamic range, and this may well prove true. Another new monomeric cyan FP, TagCFP, was derived from an avGFP-like protein from the jellyfish *Aequorea macrodactyla*. Specific details about the protein are unavailable in the literature, but it is commercially available as mammalian cloning vectors and fusions from Evrogen. The company literature reports TagCFP to be

brighter than ECFP and Cerulean, as well as similarly insensitive to physiologically relevant changes in pH.

Several additional potentially useful cyan FPs have been isolated from Anthozoan species. Derived from the reef coral *Anemonia majano*, the AmCyan1 FP [22], which is now commercially available (Clontech), has been optimized with human codons for enhanced expression in mammalian cell systems [105]. Originally named amFP486 (*Anemonia majano* FP with 486 emission maximum) in accordance with a nomenclature scheme [22] devised to simplify the discussion of myriad Anthozoan proteins, this variant exhibits a similar brightness level but a significantly better resistance to photobleaching than CFP. The absorption maximum of AmCyan1 occurs at 458 nm, whereas the fluorescence emission peak resides at 489 nm. Unfortunately, similar to most of the other reef coral proteins, AmCyan1 forms stable tetramers, which will significantly complicate attempts to employ this protein as a fusion tag or FRET biosensor.

First isolated by Miyawaki and associates from an *Acropora* stony coral species, the cyan-emitting Midoriishi-Cyan FP (abbreviated MiCy) [73] was originally designed as the donor in a new FRET combination with the monomeric Kusabira Orange FP (mKO) to generate a biosensor with high spectral overlap (Förster distance of 5.3 nm; mKO is discussed in the section on orange FPs). This protein features the longest absorption and emission wavelength profiles (472 nm and 495 nm, respectively) reported for any probe in the cyan spectral region (see Table 1.1), and similar to mTFP1, could be relegated into a new “teal” class. The high molar extinction coefficient and quantum yield exhibited by MiCy render the protein of equal brightness to Cerulean, although the fluorescence is far more sensitive to pH. Also similar to Cerulean, MiCy features a single exponential lifetime decay component with a time constant of 3.4 ns. An unusual feature of MiCy is that it forms an obligatory dimeric complex rather than the tetrameric variety observed in most coral reef species. A monomeric version of MiCy, known as mMiCy, has been mentioned in the literature [45], but details of its engineering and properties have not been reported.

Green Fluorescent Proteins

The original (wild-type) avGFP isolated from *Aequorea victoria* has been the principal subject of numerous investigations [60] but is not useful in a majority of the practical applications involving FPs due to the bimodal absorption band (395 nm and 475 nm peaks), which is hampered by relatively low extinction coefficients and an absorption maximum in the ultraviolet part of the spectrum. A point mutation replacing the serine residue at position 65 with threonine (S65T) produced a new version of the protein having a well-defined absorption

profile with a single peak at 484 nm [17]. This mutation is featured in the most popular variant of avGFP, termed enhanced avGFP (EGFP; Figure 1.1e), which can be imaged using commonly available filter sets designed for fluorescein (FITC) and is among the brightest and most photostable of any FP [3]. These features have rendered EGFP one of the most popular probes and the best choice for most single-label FP experiments.

A large number of proteins emitting in the green (~500 nm to 525 nm) spectral region have been discovered from a wide range of sources, including different *Aequorea* species [106], copepods [25], amphioxus [26], and coral reefs [22]. However, most of these FPs are naturally oligomeric, and none offers a clear advantage over EGFP. Perhaps the best current choice for live-cell imaging is the avGFP derivative Emerald (available from Invitrogen), which has properties similar to its EGFP parent [97]. Emerald (Figure 1.1f) contains the F64L and S65T mutations featured in EGFP but also has four additional point mutations that improve folding, expression at 37° C, and brightness. Although Emerald is somewhat more efficient than EGFP with respect to maturation and is slightly brighter, it has a fast photobleaching component that might affect quantitative imaging under certain experimental conditions.

The most significant addition to the green spectral region in the past several years has been coined “superfolder” avGFP [55], which is brighter and less sensitive to physiological pH changes than either EGFP or Emerald while retaining similar photostability. Therefore, the superfolder avGFP (Figure 1.1h) should be an excellent candidate for fusions with mammalian proteins, especially those that demonstrate folding problems with standard avGFP derivatives. However, because superfolder avGFP is capable of folding even when fused to insoluble proteins, the potential exists for higher background noise levels when imaging fusions in which a significant portion of the proteins fail to target correctly yet still produce bright fluorescence. In addition to the green superfolder variant, Pédelacq and co-workers also generated blue, cyan, and yellow versions by introducing the appropriate mutations at the chromophore precursor amino acid positions (for the blue and cyan variants) or position 203 (for the yellow variant). Similar to the avGFP derivative, the other superfolder colors also substantially improved fluorescence when fused to poorly folding partners in bacteria. Studies of the superfolder FPs in mammalian cells, either as a reporter for localization or gene expression, have yet to be reported.

Several of the green FP variants mined from reef corals are now commercially available (see Tables 1.1 and 1.3). A brightly fluorescent reporter termed Azami Green (Figure 1.1g; [72]), bearing only a surprisingly scant (less than 6%) sequence homology to EGFP, was isolated from the stony coral *Galaxeidae* and has been demonstrated to mature rapidly during expression in

mammalian cell lines. Likewise, one of the original Anthozoa coral reef proteins from *Zoanthus* reported by Matz and co-workers [22] has also been transformed into a commercial product (Clontech) under the name ZsGreen. The probes have absorption maxima at 492 nm and 496 nm and emission peaks at 505 nm and 506 nm, respectively, readily allowing visualization and imaging with standard lasers and filter combinations in confocal and widefield microscopy. However, similar to most of the other proteins isolated in corals, Azami Green and ZsGreen both exist as tetramers in the natural state, which significantly interferes with their use as fusion partners and as a FRET donor or acceptor in biosensors. To overcome the oligomerization problem, site-directed and random mutagenesis efforts were successful in creating a monomeric version of Azami Green (available from MBL International), but this type of effort has not been reported for ZsGreen, although the protein has been reengineered with human codons to optimize expression (resulting in a variant termed ZsGreen1). Because reliable photostability data are lacking, it is unclear whether either of these proteins will outperform EGFP in long-term imaging experiments.

Recently, two bright, monomeric GFPs derived through site-directed and random mutagenesis in combination with library screening in cyan proteins (i.e., mTFP1 and TagCFP) have been reported. Derived from *Clavularia*, mWasabi is a potential alternative green-emitting FRET partner for blue FPs [107] due to negligible absorbance at wavelengths of 400 nm and lower where blue FPs are typically excited. The new green FP is commercially available (Allele Biotechnology) and should be particularly useful in two-color imaging in conjunction with long Stokes shift proteins (such as T-Sapphire) [44] and as a localization tag in fusions with targeting proteins. A derivative of TagCFP, named TagGFP, is a bright and monomeric green variant having an absorption maximum at 482 nm and emission at 505 nm. TagGFP, which is only slightly brighter than EGFP, is available as cloning vectors and fusion tags from Evrogen but has not been thoroughly characterized in literature reports.

The sea pansy, an Anthozoa soft coral, is the source of several green FPs that have been characterized in detail [15, 108, 109]. A protein isolated from *Renilla reniformis* that exhibits properties similar to EGFP is the best characterized of the probes in this class. Having absorption and emission maxima at 485 nm and 508 nm, respectively, in addition to a similar sensitivity to pH, the *Renilla* protein would be an excellent substitute for EGFP were it not for the fact that it is an obligate dimer [37]. Aside from the oligomerization problem, *Renilla* GFPs may be useful in many applications and have been expressed in a wide variety of organisms, including bacteria, fungi, and mammalian cells. Versions with human codon sequences are available from LUX Biotechnology, as are

derivatives optimized for expression in other species. There is a general lack of reliable data concerning extinction coefficients, quantum yields, and photostability for the commercial *Renilla* proteins, so valid comparisons to EGFP in terms of brightness and photobleaching are not possible.

Yellow Fluorescent Proteins

Yellow FPs, as a spectral class, are among the most versatile genetically encoded probes yet developed. Ranging in emission wavelength maxima from approximately 525 nm to 555 nm, those proteins residing in the shorter wavelength region actually appear green, rather than yellow, when viewed in a widefield fluorescence microscope. The first member in what has become a rather large family of probes was rationally engineered after the high-resolution crystal structure of avGFP revealed that threonine residue 203 (Thr203) was positioned near the chromophore and potentially able to alter the spectral characteristics upon substitution [42]. Mutations of this aliphatic amino acid to several aromatic moieties were introduced to induce π -orbital stacking and attempt stabilization of the excited state dipole moment of the chromophore. The most successful mutant proved to be tyrosine (T203Y, the original YFP), which resulted in almost a 20-nm shift to longer wavelengths for both the excitation and emission spectra [21, 42, 60].

Several YFP variants were initially constructed to maximize brightness as well as to increase the speed of maturation and optimize expression at 37° C [60, 97]. The variants known as Citrine [92] and Venus (Figure 1.1j; [56]) are currently the most useful proteins in this spectral class (see Table 1.1), but neither is commercially available. Another variant, named after the birthstone topaz, is available from Invitrogen and has been of service in fusion tag localization, intracellular signaling, and FRET investigations [110–112]. A new member of the Evrogen “Tag” commercial series of localization reporter proteins, TagYFP, is a jellyfish-derived (*A. macrodactyla*) monomeric FP that is slightly less bright than EYFP, but an order of magnitude more photostable. Similar to the other members in the “Tag” series, TagYFP (emission peak at 524 nm) has not been characterized in the literature, but can be purchased as mammalian cloning vectors or fusion tags.

During the same FACS-based investigation that led to the generation of CyPet (discussed previously), the evolutionary optimized complementary FRET acceptor, termed YPet (Figure 1.1k), was also obtained [35]. Named after its proficiency in FRET (yellow FP for energy transfer), YPet is the brightest yellow FP variant yet developed and demonstrates very good photostability. The resistance to acidic environments afforded by YPet is superior to Venus and other YFP derivatives, which will enhance the utility of this probe in biosensor

combinations targeted at acidic organelles. However, although the optimized CyPet–YPet combination should be the preferred starting point in the development of new FRET biosensors, there remains a serious doubt as to the origin of YPet’s increased performance, which is likely due simply to enhanced dimerization with its co-evolved partner, CyPet [83, 84]. Likewise, the suitability of CyPet and YPet in fusion tags for localization experiments, bimolecular complementation analysis, and other routine FP assays has yet to be established. Both proteins exist in solution as relatively weak dimers but presumably could be converted to true monomers using the A206K mutation that has worked so well with other *Aequorea* variants.

Although the potential for new discoveries of yellow and green FPs in Hydrozoan species other than *Aequorea victoria* is significant, only a few viable candidates have surfaced so far. Isolated from the *Phialidium* jellyfish, a protein termed phiYFP [93] is reported to demonstrate very bright yellow fluorescence (absorption and emission at 525 nm and 537 nm, respectively) and to be useful for N-terminal fusion tags. An extraordinary feature of phiYFP is that the naturally occurring protein contains the same mutation at position 64 (leucine) introduced by Venus to increase the folding efficiency [56]. The probe also naturally contains tyrosine at position 203 [42], another site-directed modification of the native avGFP that resulted in yellow fluorescence. This remarkable discovery of a natural similarity between the structure of phiYFP and genetically modified *Aequorea* proteins is a testament to the efficacy of protein engineering efforts directed at avGFP to adjust the spectral properties.

Two monomeric coral reef derivatives with spectral properties falling in the range of *Aequorea* yellow FPs have been created [36]. Named after similarly colored fruits, mHoneydew and mBanana both emit fluorescence in the yellow spectral region. However, a low extinction coefficient and quantum yield render mHoneydew the dimmest member of the monomeric yellow FP cadre, and mBanana is only twice as bright as mHoneydew but features much narrower excitation and emission spectra. Because both proteins exhibit relatively poor photostability, and mBanana is highly pH-sensitive, they probably would not find great utility in imaging experiments. Perhaps the most promising aspect of these probes is that the mere existence of mHoneydew (a Y67W mutant analogous to CFP) demonstrates that the tryptophan-based chromophore of CFP can undergo a further maturation into a longer wavelength-emitting species [36].

ZsYellow (originally referred to as zFP538) is a yellow FP discovered in the Anthozoan button polyp *Zoanthus* during a search in reef corals for naturally occurring avGFP homologs emitting fluorescence in longer-wavelength regions [22, 82, 113]. One of the most unique features of the ZsYellow fluorescence emission spectrum

is that the peak (538 nm) occurs almost midway between those of EGFP (508 nm) and DsRed (583 nm), presenting an opportunity to investigate proteins emitting fluorescence in the truly yellow portion of the visible light spectrum. Unfortunately ZsYellow exhibits a marked tendency to form tetramers when expressed *in vivo*, hampering the use of this protein as a fusion partner for localization investigations. Furthermore, the reduced brightness level of ZsYellow when compared to EGFP (~25% of EGFP) also limits the utility of this FP in fluorescence microscopy. The unique emission spectral profile of ZsYellow, however, should encourage the search for genetic modifications that alleviate the tendency to form tetramers while simultaneously increasing the quantum yield and extinction coefficient, an effort that could ultimately yield a high-performance reporter. A human codon-optimized version is commercially available from Clontech as ZsYellow1.

Orange Fluorescent Proteins

In contrast to the relatively large number of FPs engineered in the cyan, green, and yellow spectral classes, only a few promising probes have been developed in the orange portion of the spectrum (ranging from ~555 nm to 590 nm). Even so, all existing orange FPs, which were isolated from coral reef species, have the potential to be useful in a variety of imaging scenarios. Perhaps the most versatile of these is monomeric Kusabira Orange (mKO) [73], a protein originally derived as a tetramer from the mushroom coral *Fungia concinna* (known in Japanese as Kusabira-Ishi). mKO (Figure 1.1) was engineered by site-specific mutagenesis from a cDNA clone of the coral by adding ten amino acids to the N-terminus. The resulting protein has an absorption maximum at 548 nm (ideal for excitation with a 543-nm laser) and emits bright orange fluorescence at 561 nm (Table 1.1). The strategy used to “monomerize” the tetrameric protein was similar to that employed for DsRed to create mRFP1 (discussed in the following) by introducing more than twenty mutations through site-directed and random mutagenesis. The monomeric mKO (commercially available from MBL International) exhibits similar spectral properties to the tetramer and has a brightness value similar to EGFP but is slightly more sensitive than the tetramer to acidic environments. The photostability of this FP, however, is among the best of any FP in all spectral classes, making mKO an excellent choice for long-term imaging experiments. Furthermore, the emission spectral profile is sufficiently well separated from cyan FPs to increase the FRET efficiency in biosensors incorporating mKO, and the probe is useful in multicolor investigations with a combination of cyan, green, yellow, and red FPs. Additional mutagenesis experiments on mKO have yielded a faster folding derivative, termed mKO2 [114], which is slightly brighter (see Table 1.1). Among

its obvious applications, mKO2 may also be useful as a FRET partner with rapidly maturing avGFP derivatives in chimeric biosensors.

The mRFP1 derivative, mOrange [36], was derived after four rounds of directed evolution to yield a probe absorbing at 548 nm and emitting orange fluorescence at 562 nm. The mOrange variant is slightly brighter than mKusabira Orange, but has less than 10% the photostability, thus severely compromising its application for experiments requiring repeated imaging. However, mOrange remains one of the brightest proteins in the orange spectral class and is still an excellent choice where intensity is more critical than long-term photostability. In addition, combined with the green-emitting T-Sapphire, mOrange is a suitable alternative to CFP–YFP proteins as a FRET pair to generate longer wavelength biosensors, and can be coupled with FPs in other spectral regions for multicolor investigations. The photostability of mOrange was recently dramatically improved with the introduction of a new strategy to utilize selective pressure for photostability in the directed evolution of FPs [115]. The resulting variant, termed mOrange2, is slightly less bright than mOrange (Table 1.1) but is approximately twenty-five times more photostable.

A novel orange FP isolated from the *Cerianthus* tube anemone [116] is commercially available (cOFP; Strata-gene) and has spectral properties similar to mOrange and mKusabira Orange, but like the other anemone proteins isolated to date, exists in solution as a tetramer. The brightness and photostability of cOFP have not been reported so this protein cannot be directly compared to other orange FPs, and its utility will be further limited until it can be converted into a monomer.

The first Anthozoa-derived FP to be extensively investigated was derived from the sea anemone *Discosoma striata* and originally referred to as drFP583, but is now commonly known as DsRed (Figure 1.1o; [22]), although the fluorescence emission is clearly more orange in color than red. Once the protein has fully matured, the emission spectrum of DsRed features a peak at 583 nm, whereas the excitation spectrum has a major peak at 558 nm and a minor peak around 500 nm. Several problems are associated with DsRed in practice. Maturation of DsRed fluorescence occurs slowly and proceeds through an intermediate chromophore stage where a majority of the fluorescence emission is seen in the green region [66]. Termed the “green state,” this artifact has proven challenging for multiple labeling experiments in combination with green FPs because of the spectral overlap. In addition, DsRed is an obligate tetramer, an undesirable characteristic that interferes in fusion protein constructs, often leading to poor localization, and increases the tendency to form large protein aggregates in living cells. Although these side effects are not important when the probe is used simply as a reporter for gene expression,

the utility of DsRed as an epitope tag is severely compromised [117]. In contrast to the large *Aequorea* family of proteins employed to successfully tag hundreds of fusion proteins, DsRed fusion proteins have proven far less successful and often exhibit toxic effects.

A bright new monomeric orange protein, named TagRFP (Figure 1.1n) and part of the Evrogen Tag series of FPs, has recently been introduced as a candidate for localization and FRET studies [118]. Derived from the dimer TurboRFP (from the sea anemone *Entacmaea quadricolor*), TagRFP was generated as a result of site-directed mutagenesis to replace several key amino acid residues involved in dimerization while simultaneously performing random mutagenesis to rescue folding properties. In total, seven rounds of semirandom mutagenesis followed by an additional round of random mutagenesis resulted in the final variant, which features excellent photophysical properties and expresses well in a wide variety of fusion tags in mammalian cells. The authors speculate that mTagRFP will be an excellent FRET acceptor when fused to green and yellow donor FPs, but that remains to be demonstrated. During the same investigation that uncovered a highly photostable variant of mOrange [115], similar mutagenesis of TagRFP yielded a single mutation (S158T) that increases the photostability almost tenfold. The resulting FP, named TagRFP-T, is perhaps the most photostable variant yet discovered.

The brightest FP in any spectral class is the tandem version of dimeric Tomato (dTomato), an orange derivative that was one of the original “Fruit” proteins (discussed in more detail in the following) [36]. This FP was derived from an intermediate termed “dimer2” obtained during the directed evolution of mRFP1, which was the first monomeric red FP reported [64], from tetrameric DsRed. The dimeric dTomato protein contains the first and last seven amino acids from avGFP on the N- and C-termini in an effort to increase the tolerance to fusion proteins and reduce potential artifacts in localization. A tandem-dimer version (effectively a “monomer”) was created by fusing two copies, head-to-tail, of dTomato with a 23-amino acid linker. Due to the presence of twin chromophores, the resulting tandem dTomato (tdTomato; Figure 1.1m) is extremely bright and has exceptional photostability. A drawback in the use of this protein is the larger size (twice that of a monomeric FP), which may interfere with fusion protein packing in some biopolymers.

Red Fluorescent Proteins

The search for an ideal red-emitting FP has long been the goal for live-cell and whole-animal imaging, primarily due to the requirement for probes in this spectral region in multicolor imaging experiments as well as the fact that longer excitation wavelengths generate less

phototoxicity and can probe deeper into biological tissues. As an added convenience, most of the proteins in this wavelength range can be imaged with the common TRITC and Texas Red fluorescence filter sets, as well as common lasers emitting spectral lines at 543 nm, 561 nm, and 594 nm in confocal microscopy. After 5 years of unsuccessful mutagenesis efforts in the avGFP-derived proteins [60], the first real breakthrough occurred with the discovery of potentially fluorescent chromoproteins in nonbioluminescent Anthozoa coral species [22]. To date, a wide spectrum of potentially useful red FPs has been reported (spanning the emission wavelength range of 590–650 nm), many of which still suffer from some degree of the obligatory quaternary structure bestowed by their species of origin (Table 1.1) [1, 3, 67]. Unlike the jellyfish proteins, most of the native and genetically engineered variants of coral reef proteins mature efficiently at 37° C, presumably due to differing water temperatures of their respective host's habitats [1].

Several major problems with DsRed FP have been overcome through site-directed and random mutagenesis efforts, but the construction of truly monomeric variants, as well as monomers from the proteins in other Anthozoa species, has proven to be a difficult task [64]. A total of thirty-three amino acid alterations to the DsRed sequence were required for the creation of the first-generation monomeric red FP (termed mRFP1) [64]. However, this derivative exhibits significantly reduced fluorescence emission compared to the native protein and photobleaches quickly, rendering it much less useful than analogous green and yellow FPs. Extensive mutagenesis research efforts [36], including newly introduced methodology, have successfully been applied in the search for yellow, orange, red, and far-red FP variants that further reduce the tendency of these potentially efficacious biological probes to self-associate while simultaneously pushing emission maxima toward longer wavelengths. The result has been improved monomeric FPs that feature increased extinction coefficients, quantum yields, and photostability, although no single variant has yet been optimized by all criteria. In addition, expression problems with obligate tetrameric red FPs are being overcome by the efforts to generate monomeric variants that are more compatible with biological function.

Perhaps the most substantial developments on this front have been the introduction of a new harvest of FPs derived from monomeric red FP (mRFP1; Figure 1.1q) through directed mutagenesis [36, 119]. The resulting cadre of monomeric FPs exhibit maxima at wavelengths ranging from 560 to 610 nm and have been named in honor of common fruits that bear colors similar to their respective fluorescence emission spectral profiles. Among the potentially efficacious members in the "fruit" series are mStrawberry (Figure 1.1p), mCherry (Figure 1.1r), and tdTomato (discussed previously), all of

which have fluorescence emission profiles in the orange and red regions of the spectrum (Table 1.1).

The red proteins, mCherry and mStrawberry (emission peaks at 610 nm and 596 nm, respectively), have brightness levels of approximately 50% and 75% of EGFP, but mCherry is far more photostable than mStrawberry and is the best probe choice to replace mRFP1 for long-term imaging experiments. A variant of mOrange, termed mApple [115], exhibits good photostability and is approximately twice as bright as mCherry (see Table 1.1), making this derivative an exceptional candidate for multicolor imaging. These new proteins essentially fill the gap between the most red-shifted jellyfish FPs (such as YPet) and the multitude of oligomeric coral reef red FPs that have been reported and are commercially available. Although several of these new fluorescent monomeric proteins lack the brightness and photostability necessary for many imaging experiments [3, 120], their existence is encouraging as it suggests the eventuality of bright, stable, monomeric FPs across the entire visible spectrum.

Further extension of the fruit protein spectral class through iterative somatic hypermutation [121] has yielded two new FPs with emission wavelength maxima of 625 nm and 649 nm, representing the first true far-red genetically engineered probes. The most potentially useful probe in this pair was named mPlum (Figure 1.1t), which has a rather limited brightness value (10% of EGFP) but excellent photostability. This monomeric probe should be useful in combination with FPs emitting in the cyan, green, yellow, and orange regions for multicolor imaging experiments and as a biosensor FRET partner with green and yellow proteins, such as Emerald and Citrine. Another far-red FP, termed AQ143, has been derived from mutagenesis efforts on a chromoprotein isolated from the anemone *Actinia equine* [122]. The excitation and emission maxima of AQ143 are 595 nm and 655 nm, respectively, and the brightness is comparable to mPlum. On the downside, the photostability of this protein has not been reported and it forms an obligate tetramer.

Several additional red FPs showing varying degrees of promise have been isolated from the reef coral organisms. One of the first to be adapted for mammalian cell applications is HcRed1 [123], which was isolated from the anemone *Heteractis crispa* and is now commercially available (Clontech). HcRed1 was originally derived from a nonfluorescent chromoprotein through site-directed and random mutagenesis to create a tetrameric red fluorescent species that matures rapidly and efficiently at 37° C (absorption and emission at 588 nm and 618 nm, respectively). Additional mutagenesis efforts resulted in a brighter dimeric variant, but a monomeric version of the protein has not yet been discovered. To generate a variant of the protein that is useful in creating fusion products for localization studies, a tandem dimer

expression vector of HcRed similar to tdTomato has been constructed [78].

A red FP, termed eqFP611, was isolated from the sea anemone *Entacmaea quadricolor* and displays one of the largest Stokes shifts and red-shifted fluorescence emission wavelength profiles (excitation and emission maxima at 559 nm and 611 nm, respectively) of any naturally occurring Anthozoan FP [124]. The quantum yield and extinction coefficient of eqFP611 combine to yield a probe approximately as bright as EGFP. In contrast to other Anthozoan FPs, eqFP611 has a reduced tendency to form oligomers at lower concentrations as evidenced through electrophoresis and single-molecule experiments [125], although at high concentrations the protein forms tetramers. Site-directed mutagenesis efforts have yielded functional dimeric variants of eqFP611 [71], and continued efforts have led to a monomeric far-red FP from this species [126].

Two additional reef coral red-emitting FPs, AsRed2 and JRed, are commercially available (Clontech and Evrogen), but these probes form tetrameric and dimeric complexes, respectively, and are less useful than the monomeric proteins described previously. AsRed2 was originally isolated as a chromoprotein from *Anemonia sulcata* [22] and modified through mutagenesis to yield a protein having an absorption maximum at 576 nm and an emission peak at 595 nm [127] with a very modest quantum yield (0.05). Although the protein has been optimized with human codons for expression in mammalian cell lines, it exhibits only about 10% the brightness level of EGFP and the photostability has not been reported. The dimeric protein, JRed, was derived through extensive mutagenesis of a jellyfish chromoprotein [93] to produce a novel red fluorescent marker with peak absorption and emission wavelengths of 584 nm and 610 nm, respectively. JRed is about 25% as bright as EGFP and exhibits limited photostability when illuminated in the 560–580 nm region, but can be successfully employed for long-term imaging experiments when excited with a 543-nm laser.

The application of site-specific and random mutagenesis to TurboRFP variants [128], followed by screening for mutations exhibiting far-red fluorescence, resulted in a dimeric protein named Katushka (emission maxima of 635 nm). Although only two-thirds as bright as EGFP, Katushka exhibits the highest brightness levels of any FP in spectral window encompassing 650–800 nm, a region important for deep tissue imaging. Introduction of the four principal Katushka mutations into TagRFP generated a monomeric, far-red protein named mKate (Figure 1.1s) that has similar spectral characteristics (Table 1.1). The photostability of mKate is reported to be exceptional and the protein displays brightness similar to that of mCherry, which makes it an excellent candidate for localization experiments in the far-red portion of the spectrum.

Large Stokes Shift Fluorescent Proteins

Mutagenesis efforts with FPs have also targeted the separation distance between absorption and emission maxima (termed the Stokes shift) to generate better probes for FRET, fluorescence cross-correlation spectroscopy (FCCS), and multicolor imaging. Substitution of isoleucine for tyrosine at position 203 (T203I) in wtGFP produces a variant, named Sapphire, that eliminates the minor excitation peak at 475 nm [60]. Sapphire exhibits an exceedingly large Stokes shift of 112 nm, with excitation and emission maxima at 399 nm and 511 nm, respectively. An optimized derivative with improved folding and brighter fluorescence, known as T-Sapphire (T for Turbo; Figure 1.1i), was constructed by introducing four additional mutations [44]. These variants should be excellent donors in FRET combinations with orange and red proteins due to their ability to be excited in the ultraviolet region.

Extending the Sapphire strategy to red FPs [45], researchers used a far more rigorous approach to construct the longest Stokes shift FP variant yet developed (180 nm) using a nonfluorescent chromoprotein derived from the *Montipora* stony coral. Mutagenesis of five residues surrounding the chromophore led to a red FP having a bimodal excitation spectrum (peaks at 452 nm and 580 nm) with emission at 606 nm. An additional four mutations substantially reduced the 580 nm peak and blue-shifted the other absorption peak to 440 nm. The resulting derivative, named Keima (after the Japanese chess piece), exhibits an emission maximum at 616 nm but is hampered in most experiments due to obligatory tetramer formation. Additional mutagenesis produced a dimer (dKeima) having similar spectral properties, and a monomer (mKeima; emission = 620 nm) was obtained after continued efforts. mKeima exhibits limited brightness (similar to the value for mPlum) and requires a specialized filter combination for imaging, but it has been demonstrated to be useful in FCCS and multicolor imaging experiments [45].

Although useful fluorophores are now available in every FP spectral class, in most cases there remains no EGFP equivalent in terms of photostability and other critical areas of performance. New additions to the blue and cyan region feature substantially improved brightness and photostability, and any of the orange FPs are excellent choices for long-term multicolor imaging. Although brighter than EGFP, photostability is still sub-optimal for most of the yellow FPs, whereas the red FPs are among the dimmest in all spectral classes. Even so, many of the FPs listed in Table 1.1 can be combined for dual- and triple-color imaging to yield excellent results. Given that most of these proteins have only been introduced in the past several years, it is highly likely that in the future, bright and photostable additions will become available for all spectral classes.

Table 1.2. A compilation of properties of the most useful optical highlighter FP reporters. Along with the common name and/or acronym for each highlighter, the peak excitation (Ex) and emission (Em) wavelengths, molar extinction coefficient (EC), quantum yield (QY), relative brightness, and physiologically relevant quaternary structure are listed for both the activated and nonactivated species. The computed brightness values were derived from the product of the molar extinction coefficient and quantum yield, divided by the value for EGFP. Photostability is not listed because little information is available on highlighter FPs. Also listed are references to the original literature sources. ^aNonactivated species

Protein (Acronym)	Ex (nm)	Em (nm)	EC × 10 ⁻³ M ⁻¹ cm ⁻¹	QY	Quaternary Structure	Relative Brightness (% of EGFP)	Reference
Photoactivatable FPs							
PA-GFP (NA) ^a	400	515	20.7	0.13	Monomer	8	[131]
PA-GFP (G)	504	517	17.4	0.79	Monomer	41	[131]
PS-CFP2 (C) ^a	400	468	43.0	0.20	Monomer	26	[136]
PS-CFP2 (G)	490	511	47.0	0.23	Monomer	32	[136]
PA-mRFP1 (R)	578	605	10.0	0.08	Monomer	3	[135]
Photoconvertible FPs							
Kaede (G) ^a	508	518	98.8	0.88	Tetramer	259	[130]
Kaede (R)	572	580	60.4	0.33	Tetramer	59	[130]
wtKikGR (G) ^a	507	517	53.7	0.70	Tetramer	112	[137]
wtKikGR (R)	583	593	35.1	0.65	Tetramer	68	[137]
mKikGR (G) ^a	505	515	49.0	0.69	Monomer	101	[139]
mKikGR (R)	580	591	28.0	0.63	Monomer	53	[139]
mEosFP (G) ^a	505	516	67.2	0.64	Monomer	128	[74]
mEosFP (R)	569	581	37.0	0.62	Monomer	68	[74]
mEos2FP (G) ^a	506	519	56.0	0.84	Monomer	140	[140]
mEos2FP (R)	573	584	46.0	0.66	Monomer	90	[140]
tdEosFP (G) ^a	506	516	84.0	0.66	Monomer	165	[79]
tdEosFP (R)	569	581	33.0	0.60	Monomer	59	[79]
Dendra2 (G) ^a	490	507	45.0	0.50	Monomer	67	[75]
Dendra2 (R)	553	573	35.0	0.55	Monomer	57	[75]
Photoswitchable FPs							
Kindling – KFP1 (R)	580	600	59.0	0.07	Tetramer	12	[132]
Dronpa (G)	503	518	95.0	0.85	Monomer	240	[76]

OPTICAL HIGHLIGHTERS: TOOLS FOR THE STUDY OF PROTEIN DYNAMICS

A special class of FPs known as “optical highlighters” includes a subset of the color palette with photophysical characteristics that enable the activation or conversion of fluorescent properties by controlled illumination [11, 129]. Table 1.2 presents a compilation of physical data for the current palette of optical highlighter FPs that display significant potential in applications as *in vivo* probes targeting cellular structure and function. Optical highlighters can be further divided into three classes based on whether they are photoactivated, photoconverted, or photoswitched. FPs that can be activated to initiate fluorescence emission from a dark or quiescent state are termed “photoactivatable,” whereas those that can

be optically converted from one fluorescence emission bandwidth to another are “photoconvertible.” A third class, FPs that can be reversibly toggled between dark and light states, is referred to as “photoswitchable.” Synthetic fluorophores with optical highlighter-like properties have been known for decades, but these attributes have only recently been discovered in genetically encoded FPs [130–132]. Photoactivated FPs generally exhibit little or no initial fluorescence under excitation at the imaging wavelength, but dramatically increase their fluorescence intensity after activation by irradiation at a different (usually lower) wavelength (Figure 1.9). In contrast, photoconversion involves a change in the fluorescence emission bandwidth profile (generally from shorter to longer wavelengths) upon optically induced changes to the FP chromophore. Photoswitchable FPs can be turned

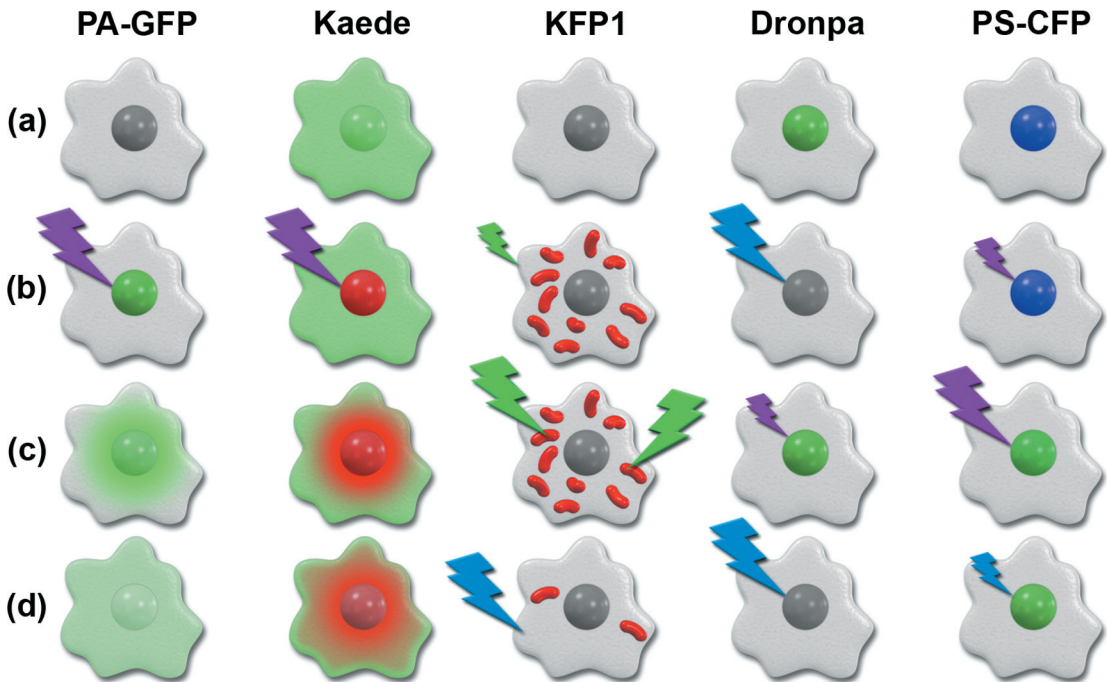


Figure 1.9. Cartoons illustrating the photoconversion mechanisms for the most useful optical highlighters developed to date. The photoactivation, photoconversion, or photoswitching sequence for each highlighter is outlined in a single column, with a repetitive cartoon drawing representing an individual cell containing a central nucleus being employed for each step in the sequence. Illumination at high intensities (photoconversion light levels) is indicated by large lightning bolts, while low-intensity illumination (imaging light levels) is represented by smaller bolts. The fluorescence excitation wavelengths are similar to the colors of the lightning bolts, whereas the emission colors appear in the nucleus and/or cytoplasm of the cell cartoons. To examine a sequence, start with the uppermost cell drawing and proceed down the column. For example, a single cell containing photoactivatable green fluorescent protein (PA-GFP) before conversion is illustrated at the top of the first column and appears nonfluorescent (grayscale). After illumination of the nucleus with 405-nm light (purple lightning bolt), the PA-GFP protein exhibits green fluorescence throughout the nucleus, which slowly diffuses into the cytoplasm, as illustrated by the lower two cell cartoons ((C) and (D)) in the first column. The other columns contain sequences that symbolize the photoconversion mechanisms for selected optical highlighters. A cell expressing green fluorescent native Kaede (second column) is photoconverted to red in the nuclear region, which slowly diffuses into the cytoplasm. Highlighting mitochondria with KFP1 (third column) enables these organelles to be visualized transiently or permanently, whereas Dronpa (fourth column) can be turned on and off with alternating 488- and 405-nm lasers. PS-CFP (fifth column) can be visualized with weak 405-nm illumination or photoconverted from cyan to green with intense 405-nm illumination.

“on” or “off,” in some cases with timescales in the millisecond range, by simply changing the illumination wavelength. Optical highlighters represent perhaps the most promising approach to the *in vivo* investigation of protein dynamics [11] and have recently become useful for high-resolution microscopy techniques that break the classical diffraction barrier [133, 134].

The ideal optical highlighter FP should be readily photoconvertible or photoactivatable (through the process of fluorescence activation and/or emission wavelength shifts) to produce a high level of contrast. It should also be monomeric for optimum expression in the target system. These probes will be especially useful in experiments paralleling results obtained with photobleaching techniques, such as recovery (FRAP) and loss (FLIP) of photobleaching, because they have the advantage that measurements are not influenced by newly synthesized or nonconverted proteins, which either remain invisible or

continue to emit the original wavelengths [11]. Also, by repeated excitation in the region of interest, optical highlighters can be continuously photoconverted at a specific intracellular location. This technique is more efficient than FLIP because the translocation of activated proteins can be directly imaged. In addition, time required for photoactivation (a few seconds) is often much less than the time required to completely photobleach a similar region. Investigations involving extremely rapid cellular processes will clearly benefit from such improvements in temporal resolution.

Photoactivatable Fluorescent Proteins

The first useful optical highlighter designed specifically for photoactivation studies is a variant of avGFP, termed PA-GFP (Figure 1.10a–c). This photoactivatable version of avGFP was developed by improving on the

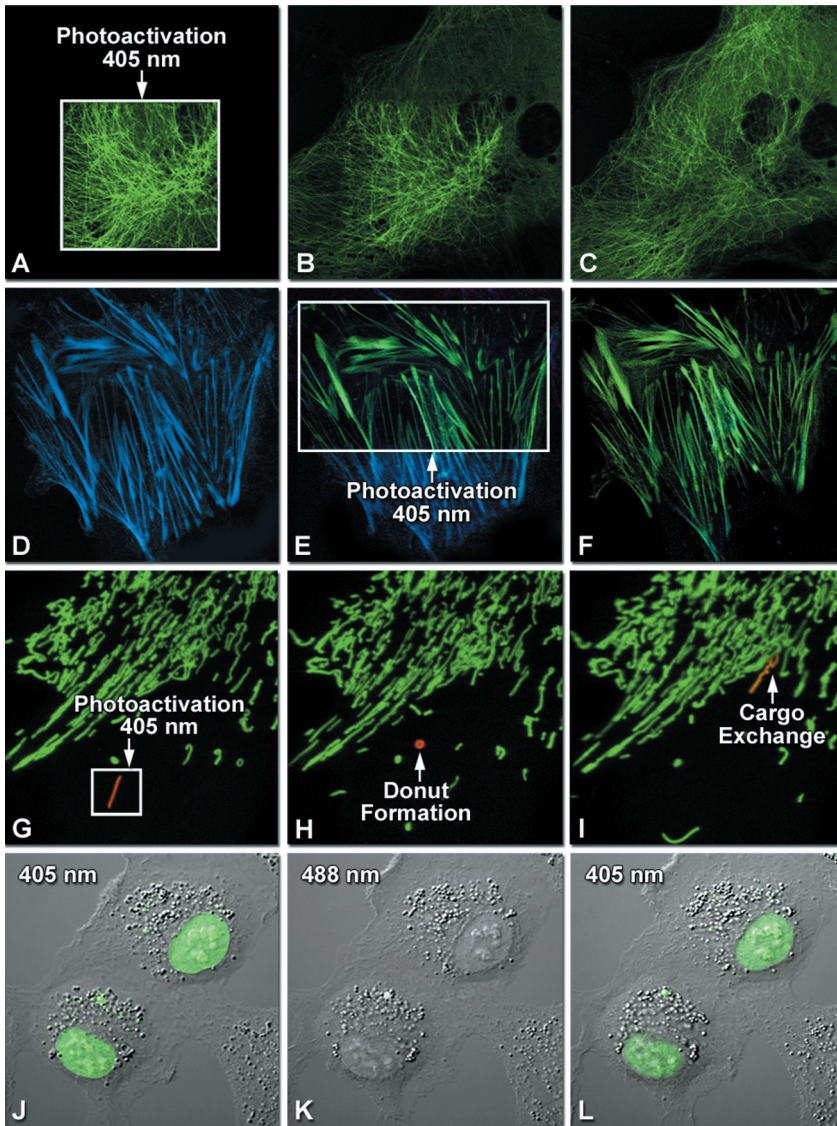


Figure 1.10. Optical highlighter FP reporters in action imaged with laser scanning confocal microscopy. **A–C:** Photoactivation of mPA-GFP-tubulin-C-6 in normal African green monkey kidney (CV-1 cell line) fibroblast cells; **(A)** Rectangular region of interest (white box) selected with Olympus FV1000 SIM scanner is illuminated at 405 nm for 5 sec, $t = 0$; **(B)** The photoactivated tubulin chimera initially translocates to microtubules throughout the cytoplasm as fluorescence intensity decreases in the activated region, $t = 15$ min; **(C)** The microtubule network gains more intensity at $t = 60$ min. **D–F:** Photoconversion of PS-CFP2-actin-C-7 in gray fox lung (FoLu cell line) fibroblast cells; **(D)** Single FoLu cell expressing the actin chimera imaged with a 405-nm laser; **(E)** Photoconversion of labeled actin filaments in the lower portion of the viewfield in a selected region of interest (white box) with 405 nm illumination at $t = 0$; **(F)** Photoconverted PS-CFP2 in the actin chimera has translocated into most of the filaments at $t = 30$ min. **G–I:** Tracking of mitochondria labeled with tdEos-mito-N-7 in rabbit kidney (RK-13 cell line) epithelial cells; **(G)** Photoconversion of a single mitochondrion (red) in a selected region (white box) with 405 nm illumination at $t = 0$; **(H)** Formation of a donut by the photoconverted mitochondrion at $t = 2$ min; **(I)** Cargo exchange between mitochondria (arrow) at $t = 3$ min. **J–L:** Photoswitching of the histone H2B with Dronpa-H2B-N-6 in opossum kidney (OK cell line) epithelial cells; **(J)** Labeled nuclei in adjacent cells imaged with 488 nm laser with differential interference contrast, $t = 0$; **(K)** After completely photoswitching the labeled histones “off” at 488 nm, the nuclei now appear devoid of fluorescence, $t = 3$ min; **(L)** Dronpa label in nucleus, reactivated with illumination at 405 nm, appears dimmer due to photobleaching after forty rounds of photoswitching.

photoconversion efficiency of the natural wild-type protein chromophore from a predominately neutral form to a species that is anionic in character [131]. Substitution of histidine for threonine at position 203 (T203H) produced a variant with negligible absorbance in the region between 450 nm and 550 nm, thus enhancing the contrast between the nonactivated and activated species. After photoactivation with violet light (~405 nm), the absorption maximum at 504 nm in PA-GFP increases approximately 100-fold. This event evokes high contrast differences between the converted and unconverted pools of PA-GFP and is useful for tracking the dynamics of molecular subpopulations within a cell (Figure 1.9, Column 1). On the downside, intracellular targets expressing PA-GFP are not easily distinguishable prior to being photoactivated, thus making the definition of regions for observation difficult.

Several new photoactivatable proteins have been produced using site-directed mutagenesis of a monomeric red-shifted reef coral FP. The monomeric derivative of DsRed FP, mRFP1, has been converted to a probe photoactivated by either green or violet irradiation [135]. This FP, termed PA-mRFP1, exhibits a 70-fold increase of fluorescence intensity upon activation by wavelengths between 380–400 nm. Unfortunately, the relatively low level of fluorescence intensity of PA-mRFP1 in the photoactivated form (3 percent of EGFP) renders it significantly less useful than PA-GFP for live-cell investigations. Clearly, this class of optical highlighters would benefit from efforts to engineer the mFruit proteins (such as mCherry and mPlum) into photoactivatable probes.

A novel photoconvertible optical highlighter, termed photoswitchable cyan FP (PS-CFP2; Figure 1.10d–f), derived from the *Aequorea coerulescens* green FP variant, aceGFP, has been observed to transition from cyan-to-green fluorescence upon illumination at 405 nm (Figure 1.9, Column 5). The PS-CFP2 highlighter was generated by site-directed mutagenesis of aceGFP [136] and is expressed as a monomer *in vivo*. Among the advantages of PS-CFP2 is the significant level of cyan fluorescence present before photoconversion, a factor that allows investigators to track and selectively illuminate specific intracellular regions or entire cells for study. However, the dynamic range of PS-CFP2 is significantly lower than that of PA-GFP, and the probe is inferior to highlighters in the green-to-red spectral class in terms of photoconversion efficiency.

Photoconvertible Fluorescent Proteins

Several potentially useful green-to-red photoconvertible optical highlighters have been developed in FPs cloned from reef coral and sea anemone species. One of the first and most important examples, a tetrameric FP isolated from the stony Open Brain coral, *Trachyphyllia geoffroyi*, has been found to photoconvert from green

to red fluorescence emission in ultraviolet light (Figure 1.9, Column 2; [130]). The unusual color transition prompted investigators to name the protein Kaede after the leaves of the Japanese maple tree, which turn from green to red in the fall months. Illumination of Kaede with ultraviolet or violet light results in a spectral shift of the native (green) species from 508 nm (absorption) and 518 nm (emission) to longer wavelength peaks at 572 nm and 582 nm, respectively. Upon photoconversion, Kaede exhibits a dramatic increase in the red-to-green fluorescence ratio (approximately 2000-fold, considering both the decrease in green and the increase in red emission). The photoconversion is stable and irreversible under aerobic conditions, and the red fluorescent state of the Kaede chromophore is comparable to the green in terms of brightness and photostability.

The stony coral *Favia favaus* has yielded a promising tetrameric derivative that exhibits efficient photoconversion from green to red fluorescence emission wavelengths (similar to Kaede) upon irradiation with near-ultraviolet or violet light [137]. Engineering efforts based on structural analysis of this protein produced a variant, termed KikGR, which is several-fold brighter than Kaede in both the green and red states and features a wider separation of green and red emission maxima than Kaede (75 nm vs. 54 nm). Another tetrameric stony coral FP, EosFP, emits bright green fluorescence at 516 nm that shifts to orange–red (581 nm) when illuminated with light at wavelengths in the near-ultraviolet region of 390–405 nm [74]. Two single point mutations have been employed to split the wild-type tetramer into dimeric subunits and a combination of both single point mutations yields a true monomeric protein (mEosFP). The monomer can be incorporated into functional biological chimeras to serve as a marker in live-cell imaging [138], although the monomer fusions are only efficiently expressed at temperatures below 30° C (limiting their applications in mammalian systems). An EosFP tandem dimer (Figure 1.10g–i; [74, 79]) exhibits far better maturation at 37° C and is much brighter, making this variant one of the best choices in its spectral class. Recently, monomeric versions of KikGR [139] and Eos (mEos2; [140]) have been reported. Initial studies using both of these derivatives (Davidson, unpublished) indicate that they have significant potential in a wide variety of fusions for investigations of live-cell dynamics and superresolution microscopy.

The first useful monomeric green-to-red photoconvertible FP was derived from a soft coral and originally named Dendra [75] but was shortly followed by an improved commercial version (Evrogen) known as Dendra2. Capable of being photoconverted by ultraviolet, violet, and blue wavelengths (in decreasing order of effectiveness), Dendra2 exhibits a high dynamic range (up to 4000) and matures rapidly at 37° C. The monomeric nature of Dendra2 makes this FP ideal for sensitive

fusions and FRET investigations, and the ability to photoconvert with a common argon-ion laser at 488 nm reduces the phototoxic effects induced by shorter wavelengths. On the downside, the green species of Dendra2 is less than half as bright as the tetrameric analogs or tandem dimer EosFP, and the photoconverted species may not be as photostable as originally reported.

Other proteins similar to Kaede, KikGR, Dendra2, and EosFP that are capable of being photoconverted by violet and ultraviolet illumination have been discovered in the Great Star coral (mcaVRFP) and the mushroom coral (rflorFP) [23]. All of these highlighters contain a common chromophore derived from the tripeptide His-Tyr-Gly (HYG) that initially emits green fluorescence until driven into a red state by strong ultraviolet illumination. Irradiation induces cleavage between the amide nitrogen and *alpha* carbon atom in the histidine residue with subsequent formation of a highly conjugated dual imidazole ring system, a process requiring catalysis by the intact protein and resulting in the dramatic shift of fluorescence emission to red wavelengths [141, 142]. The unconventional chemistry involved in this chromophore transition should give engineers an excellent foundation upon which to develop more advanced highlighters.

Photoswitchable Fluorescent Proteins

Although the phenomenon of photochromism (the ability to switch fluorescence on and off) has been observed in the wild-type and several yellow FP derivatives of avGFP at the single molecule level [143, 144], none has demonstrated this phenomenon when measured in bulk. In these studies, during illumination at 488 nm, the molecules exhibited fluorescence for several seconds, followed by an equally short time interval without emission, followed later by resumption of emission. Termed blinking behavior [145], this on-and-off switching sequence can be repeated a number of times before each avGFP molecule ultimately photobleaches. Unfortunately, photoswitching in most of the FPs described previously cannot be done successfully in quantitative experiments.

A new generation of specialized optical highlighters with reversible on-off switching capabilities was created by the introduction of Dronpa (Figure 1.10j)–l), a monomeric FP derived from the *Pectiniidae* coral [76]. Named after a fusion of the ninja term for vanishing (dron) and photoactivation (pa), Dronpa exhibits unusual behavior due to its ability to toggle fluorescence on and off by illumination with two different wavelengths (Figure 1.9, Column 4). Dronpa was engineered using both directed and random mutagenesis to yield a monomeric version of the wild-type oligomeric FP having a major absorption maximum at 503 nm and a minor peak at 390 nm. The absorption peak at 503 nm is due to the deprotonated species of the protein, whereas the smaller peak at 390 nm arises from the protonated form.

When irradiated at 488 nm, the fluorescence emission of the deprotonated species has a maximum at 518 nm with a relatively high quantum yield of 0.85 (Table 1.2). In contrast, the protonated form of the protein is almost nonfluorescent. Photoswitching of Dronpa occurs by interconversion between the deprotonated and protonated forms [146]. Upon irradiation at 488 nm, Dronpa is driven to the protonated species with a commitment decrease in fluorescence to produce a dim (off) state in which the 390-nm absorption peak predominates. The dim state is readily converted to the original fluorescent (on) deprotonated state with minimal illumination at 405 nm. Similar behavior has been reported for a teal FP, termed mTFP0.7 [40], in which the dark and fluorescent states have been characterized by crystallography.

Another potentially useful photoswitchable optical highlighter, the Kindling FP (KFP1), has been developed from a nonfluorescent chromoprotein isolated in *Anemonia sulcata* [23, 132, 147] and is now commercially available (Evrogen). Kindling FP does not exhibit emission until illuminated with green or yellow light in the region between 525 nm and 580 nm. Low-intensity light results in transient red fluorescence (kindling) with excitation and emission maxima at 580 nm and 600 nm, respectively, which slowly decays in the dark as the protein relaxes to its initial nonfluorescent state. Irradiation with intense blue light quenches the kindled fluorescence immediately and completely, allowing tight control over fluorescent labeling (Figure 1.9, Column 3). Note that both kindling with low-intensity green light and quenching of fluorescence by blue light are reversible processes for the wild-type protein. In contrast, high-intensity illumination or continued irradiation at moderate levels results in irreversible kindling with a fluorescence intensity approximately 30-fold greater than that of the nonactivated protein. Irreversibly kindled molecules do not lose their fluorescence and are not quenched by illumination with blue light. This feature allows for stable long-term highlighting of cells, tissues, and organelles similar to PA-GFP and other highlighter proteins. The major drawback of kindling protein is its tendency to aggregate into tetramers, which seriously affects the potential for use as a protein fusion tag without some degree of disturbance to normal biological processes. However, the kindling protein is an excellent candidate for bulk photolabeling and tracking of individual organelles and cells within a large population.

Investigations into the underlying mechanism of FP photoswitching [40, 148–151] suggest that *cis-trans* isomerization of the tyrosine chromophore is a key event in the process. The *cis* conformation represents the bright fluorescent state, whereas the *trans* isomer is adopted by the chromophore in the nonfluorescent, or dark, state. The conformational changes are thought to be accompanied by varied chromophore protonation states that also contribute to the determination of the fluorescent

properties. Furthermore, photoswitching is probably a manifestation of chromophore planarity and structural rearrangements of internal amino acid side chains within the chromophore cavity. These collective features may constitute a fundamental mechanism common to all photoactivatable and reversibly photoswitchable FP derivatives.

The potential for optical highlighters remains far greater than the current realization of useful derivatives in this category. Among the photoactivatable probes, PA-GFP is still the best choice and is far superior in terms of dynamic range to the only red variant yet reported, PA-mRFP1 [135]. The only choice for cyan-to-green photoconversion, PS-CFP2 [136], exhibits monomeric character but is compromised by low brightness levels and the artifact of continued photoconversion during imaging. In the green-to-red class, the best performers in terms of brightness and conversion efficiency are tetramers. Thus, they are not useful for a majority of experiments. The monomeric variant, Dendra2 [75], is probably the best choice for fusions and FRET studies but suffers from rapid photobleaching of the red species and is less than half as bright as the tetramers. A tandem dimer of the green-to-red highlighter named EosFP [74, 79] behaves better than Dendra2 in terms of brightness and photostability, but is twice as large. Clearly, there is a significant need for better performers in all of the optical highlighter categories.

ADDITIONAL PRACTICAL CONSIDERATIONS

Recent advances in FP technology have turned many biologists into experts in live-cell imaging and microscopy. Investigators who want to track their favorite protein simply fuse the gene to the cDNA for an FP of choice and transfer the resulting recombinant vector into a host cell or whole organism. In the best cases, the new chimera enables the host protein to be normally involved in its routine cellular duties while the piggyback FP contributes a fluorescent molecular beacon to report on the position of the conjoined pair. FRET biosensors are slightly more complicated, but the general aspects are the same. Unfortunately, the best case scenario is not universally observed in practice, leaving the investigator puzzled over whether a different FP would produce the optimum result.

Assuming the host cells are initially in log phase and healthy, and provided the transfection protocol does not produce excessive levels of trauma, the most common problems encountered in working with FPs are aggregation, incorrect localization, nonfunctional fusions, and suppression of the expected fluorescence intensity. Once these problems are corrected, the investigator must choose between examining the cells in transient FP

transfections, where expression levels are highly varied, or in taking more time to select stably expressing cell populations that often produce superior results. It is often tempting (and much quicker) to transiently express the FP fusion and search for cells exhibiting low levels of fluorescence intensity that may correspond to expression levels minute enough to not interfere with normal function (see Figure 1.11). However, producing stable cell lines presents an opportunity for a quantitative comparison of fusion expression to that of the endogenous protein and is a much safer bet. Alternatively, placing the fusion construct into a vector having an inducible promoter enables control in modulating the level of expression.

In some cases, the FP fusion exhibits unexpectedly low levels of fluorescence when expressed. This problem can be due to a number of factors, including the localized environment (primarily pH) of the target organelle, improper folding of the chimera, lack of expression, or a highly unstable fusion complex. Many organelles have internal pH ranges that differ widely from that of the cytoplasm, and this can interfere with FP detection in some fusions. Successfully targeting FPs to the Golgi, endosomes, lysosomes, secretory granules, and other acidic organelles requires the use of FPs with relatively low pKa values. For example, EGFP and Venus are more likely to experience a loss of fluorescence in the lumen of the Golgi complex than is TagRFP, which has a much lower pKa. In general, fine-tuning the target environment with suitable FP parameters will ensure that intensity problems must be assigned to other variables.

Improper folding of either the FP, the host fusion protein, or the entire chimeric complex is another source of poor fluorescence intensity. Provided each of these entities folds properly when expressed separately, the first candidate for examination is the linker between the FP and its host, which should be optimized for every application. If the linker is not sufficiently long and flexible enough to separate the two protein domains, steric hindrance can lead to folding interference in one or both of the proteins. The first choice for linker components is the amino acid glycine, which has the smallest side chain and bestows the greatest degree of flexibility to any peptide. Interspersing several glycine residues with serine improves solubility and should be considered for longer linkers. Additionally, the use of many other amino acids in FP fusion linkers has been reported, indicating that there is a wide tolerance to residue choice. Usually, a linker length between two and ten amino acids is sufficient, but the optimum size also depends upon whether the fusion occurs at the amino (N) or carboxy (C) terminus of the FP. EGFP and other avGFP variants have a flexible C-terminal stretch of approximately ten amino acids, which considerably shortens the required linker length. In contrast, the N-terminal region of these probes is much less tolerant to fusions and requires a longer linker. The opposite is true for several coral FPs, but the

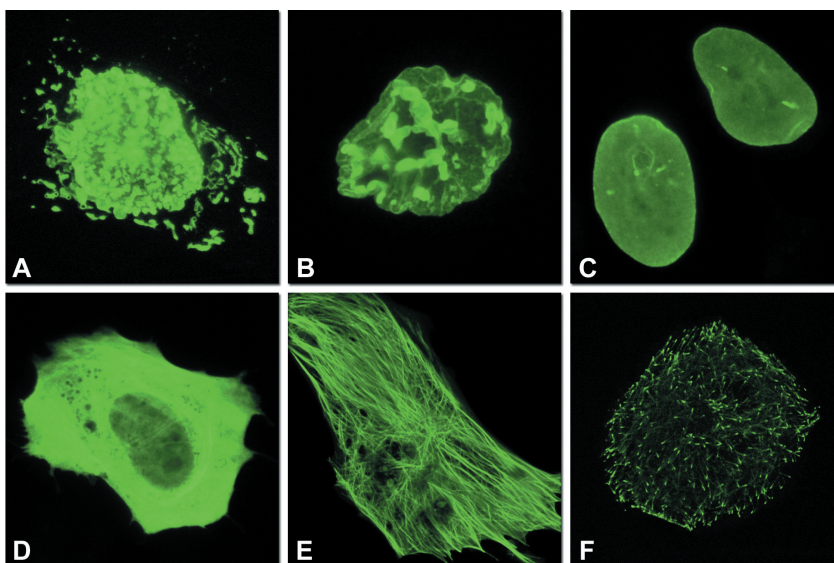


Figure 1.11. Varied FP expression levels in transient transfections. **A–C:** mEmerald-lamin B1-C-10 expressed in HeLa cells; **(A)** Extreme overexpression is manifested by FP background fluorescence in the Golgi complex, aggregates in the nucleus, and distortion of nuclear envelope structures; **(B)** Moderate overexpression distorts the nucleus and produces aggregates in the nucleoplasm and nuclear envelope; **(C)** Low expression levels exhibit evenly distributed lamin fusion protein and distinct foci that inhabit the nucleoplasm; **D–F:** mEGFP-EB3-N-7 expressed in Gray fox lung (FoLu cell line) fibroblast cells; **(D)** Extreme overexpression pervades the cytoplasm with little definition of microtubules, but the fusion protein is apparently too large to enter the nucleus; **(E)** Moderate overexpression resembles outlines in the microtubule network, but individual (+) ends are obscured; **(F)** Low expression levels clearly reveal defined EB3-labeled microtubule (+) termini, which can be followed as they migrate through the cytoplasm with time-lapse imaging. Stable transfectants should be selected from cells expressing FP fusions at levels similar to those represented in **(C)** and **(F)**. Images were pseudocolored to correspond to the respective FP emission wavelength maximum.

crystal structure for many proteins remains undetermined, so the investigator should err on the side of caution and choose longer linkers in the absence of structural data.

In cases where the FP fusion is not expressed or is highly unstable, the focus of troubleshooting efforts should be on the position of the fusion or the molecular integrity of the construct. If the protein is expressed but unstable, the chimera will often perform better if the FP is placed in a different position, such as the N-terminus when the C-terminal fusion behaves poorly. Although rare, some host proteins will not tolerate a FP fusion to either end, leaving only the choice of inserting the probe somewhere in the middle of the host sequence. The most tolerant regions are highly flexible loops, but other sequences where the amino acids are relatively disordered may work as well. Another possibility is to use circularly permuted FP derivatives [152, 153] where the original amino and carboxy termini have been linked with a short spacer and new terminal ends established within the β -barrel. A total lack of expression usually indicates a problem with the construct design (such as the FP being inserted out of frame). After ensuring that the nucleotide sequence is correct and contains a Kozak initiation site, check to determine if the flanking sequences of the fusion gene may be interfering with transcription

or translation. The remedy may be to excise the entire fusion gene and insert it into a multiple cloning site of a standardized expression vector.

Poor localization, which can occur for a variety of reasons, is perhaps the single largest source of problems when examining FP fusion chimeras. In many cases, the primary cause is interference with the host protein's normal biological function, but aggregation and oligomerization artifacts from the FP itself, as well as excessively high expression levels, can also produce the same result (see Figures 1.11 and 1.12). The same approach of checking fusion termini and modulating linker lengths discussed previously is the first place to start in troubleshooting localization problems, provided the FP is believed to be monomeric and does not aggregate when expressed alone. In situations where the fusion host protein itself forms a biopolymer or intermolecular complex (such as actin, tubulin, and the histones), any degree of oligomerization can be disruptive to proper localization and should be suspected. In general, many newly developed monomeric orange and red proteins from coral species should be suspected of contributing artifacts if aggregation or improper localization is observed. The best approach when using these FPs is to compare the distribution of new fusion chimeras with the distribution of the native protein fused to a well-studied EGFP

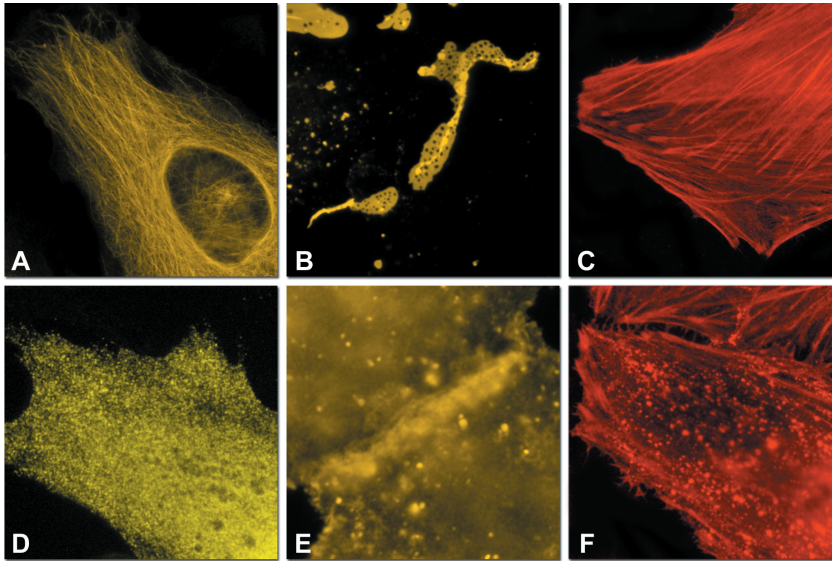


Figure 1.12. Examples of good and poor localization and cytoplasmic aggregation artifacts. **(A)** mTagRFP-tubulin-C-6 in HeLa cells demonstrates excellent morphology in defining the microtubule network; **(D)** mKO-tubulin-C-6 in HeLa cells displays much poorer localization than the identical mTagRFP construct; **(B)** mTagRFP-Cx43-N-7 forms well-defined gap junctions in HeLa cells; **(F)** tdTomato-Cx43-N-7 forms inferior gap junctions and is difficult to distinguish from overlapping cell membranes; **(C)** mPlum-actin-C-7 localizes very nicely to the filamentous network in many cases, but can also form aggregates throughout the cytoplasm **(G)**, often centered around the nucleus in the area of the Golgi complex. Images were pseudocolored to correspond to the respective FP emission wavelength maximum.

variant or to subsequently verify proper localization using immunofluorescence.

A final note on applying new FP variants in fusion constructs serves to underscore the fact that expression levels can often be maximized by redesigning the nucleic acid sequence to coincide with codon preferences of the host organism [68]. Neither the native jellyfish nor coral reef native codon usage is optimal for mammalian cells, and translation of any protein in eukaryotes can be further assisted by including the proper initiation sequence [154]. Installing a new codon beginning with a G immediately after the start codon (Met, ATG) is sufficient to produce the Kozak site but introduces an extra amino acid (preferably Val or Ala) into the sequence. In avGFP variants the N-terminal region is tolerant to such additions, but the same may not hold true for other FPs.

Commercial Availability

Obtaining new FPs is often a major impediment to investigators who want to begin work in this area or transition into multicolor imaging experiments. Fortunately, many variants listed in Tables 1.1 and 1.2 are now available through commercial distributors, and new FPs are continuously being added to their existing inventories. Table 1.3 lists the current (spring 2009) choices for commercial sources of FPs. These probes are usually available as plasmid “cloning” vectors that have been optimized with silent base-pair changes to generate codons ideal

for mammalian or bacterial expression and often contain the Kozak sequence. Cloning vectors contain a specialized region of 80–100 nucleotides, termed a “multiple cloning” site (MCS) positioned either N- or C-terminal to the FP, which houses a host of popular restriction endonuclease sites for convenient insertion of fusion host proteins. Genes inserted into the MCS will be expressed as fusions provided they are in the same reading frame as the FP and there are no intervening stop codons. Other features common to many commercial cloning vectors include a polyadenylation signal downstream of the fusion site to aid in processing of the 3' terminus of the fusion mRNA and origins of replication for both bacterial and mammalian hosts. Antibiotic resistance cassettes are usually included to allow for selection in bacteria with kanamycin or ampicillin and in mammalian cells with G-418 or another antibiotic.

FLUORESCENT PROTEIN APPLICATIONS

Initially, FPs were used almost exclusively for targeting fusions to specific subcellular locations using proteins and signal peptides in mammalian cell cultures, a task for which they are well suited. However, as FP technology has matured, these ubiquitous fluorescent probes are finding uses in an increasing number of applications as diverse as superresolution microscopy [133, 155, 156], single-molecule imaging [157, 158], neurobiology

Table 1.3. Commercial Sources of FP and Optical Highlighter Vectors

<i>Company Name</i>	<i>Web Site Address</i>	<i>Postal Address</i>	<i>Contact Information</i>	<i>Fluorescent Protein Products</i>
Addgene	http://www.addgene.org	Addgene Inc. 1 Kendall Square Cambridge, MA 02139 USA	Tel: (617) 225-9000 Fax: (888) 734-0533 E-mail: info@addgene.org	Nonprofit plasmid archive for research scientists. Distributes numerous fluorescent protein vectors
Allele Biotechnology	http://www.allelebiotech.com	Allele Biotech 9924 Mesa Rim Road San Diego, CA 92121 USA	Tel: (858) 587-6645 Toll Free: 800 991-7624 Fax: (858) 587-6692 E-mail: oligo@allelebiotech.com	Alleleustrous Line: mTFP1, mWasabi
Amaya Biosystems	http://www.amaya.com	Amaya Inc. 205 Perry Parkway, Suite 7 Gaithersburg, MD 20877 USA	Tel: (888) 632-9110	Amaya pmaxFP Line: pmaxFP-Green, pmaxFP-Yellow, pmaxFP-Yellow-m, pmaxFP-Red.
BD Biosciences	http://www.bdbiosciences.com	BD Biosciences 2350 Qume Drive San Jose, CA 95131 USA	Tel: (877) 232-8995 Fax: (800) 325-9637 E-mail: facservice@bd.com	Baculovirus Transfer Vectors with BFP and YFP variants
Clontech Laboratories	http://www.clontech.com	Clontech Laboratories, Inc. 1290 Terra Bella Ave. Mountain View, CA 94043 USA	Tel: (800) 662-2566 Fax: (800) 424-1350 E-mail: orders@clontech.com	Living Colors Line: AcGFP1, AmCyan1, AsRed2, DsRed2, DsRed-Express, DsRed-Monomer, HcRed1, ZsGreen1, ZsYellow1, mFruits
Evrogen	http://www.evrogen.com	Evrogen Joint Stock Company Miklukho-Maklaya str, 16/10, 117997, Moscow, Russia	Tel: +7(495) 429-8020 Fax: +7(495) 429-8520 E-mail: evrogen@evrogen.com	Turbo and Tag Line: TurboGFP, YFP, RFP, FP602TagCFP, GFP, YFP, RFP; PhiYFP, JRed, PS-CFP2, Dendra2, KFP-Red, HyPer, KillerRed
Invitrogen	http://www.invitrogen.com	Invitrogen Corporation 1600 Faraday Avenue Carlsbad, CA 92008 USA	Tel: (760) 603-7200 Fax: (760) 602-6500 E-mail: catalog@invitrogen.com	Vivd Colors Line: Emerald, Topaz, CFP, BFP Cycle 3 GFP
LUX Biotechnology	http://luxbiotech.com	LUX Biotechnology Ltd BioSpace, King's Buildings Edinburgh United Kingdom EH9 3JF	Tel: +44(0)131-662-3350 Fax: +44(0)131-662-3396	NanoLight Line (UK): <i>Renilla Mullerei</i> GFP, <i>Ptilosarcus</i> GFP, <i>Renilla Reniformis</i> GFP
MBL International Corporation	http://www.mblintl.com	MBL International 15 B Constitution Way Woburn, MA 01801 USA	Tel: 800 200-5459 Fax: (781) 939-6963 E-mail: info@mblintl.com	CoralHue Line: mAzami Green, mKusabira Orange, Dronpa, Kaede, Kikume Green-Red, Keima Red, Midoriishi-Cyan,
NanoLight Technology	http://www.nanolight.com	Bruce Bryan, MD 163 W. White Mountain Blvd. Pinetop, AZ 85935 USA	Tel: (928) 367-1200 Fax: (928) 367-1205 Lab Tel: (928) 333-2001 E-mail: bruce@prolume.com	NanoLight Line (USA): <i>Renilla Mullerei</i> GFP, <i>Ptilosarcus</i> GFP, <i>Renilla Reniformis</i> GFP
PerkinElmer	http://las.perkinelmer.com	PerkinElmer Life and Analytical Sciences 940 Winter Street Waltham, MA 02451 USA	Tel: (781) 663-6900 E-mail: customer-careus@perkinelmer.com	BRET ² Assay Vectors Line: GFP ² Humanized Codon Cloning Vectors
Promega	http://www.promega.com	Promega Corporation 2800 Woods Hollow Road Madison, WI 53711 USA	Tel: 608-274-4330 Fax: 608-277-2516 E-mail: custserv@promega.com	Monster Green Line: phMGFP
Stratagene	http://www.stratagene.com	Stratagene 11011 N. Torrey Pines Road La Jolla, CA 92037 USA	Tel: (858) 373-6300	Vitality Vectors: hrGFP and hrGFP ^{II} Nuc, Mito, Golgi, Peroxy

[9, 159], visualization of mRNA localization and trafficking [160, 161], FRET biosensors [162–164], bioluminescence resonance energy transfer or BRET [165–167], plant cell biology [168–170], bimolecular fluorescence complementation [171, 172], fluorescence correlation spectroscopy [173], *in vivo* imaging [174–176], drug discovery [177, 178], and in correlative morphological investigations of optical fluorescence techniques in combination with electron microscopy [29, 179].

The combined methodologies being developed with the aid of FPs are impressive and will no doubt continue to expand in the coming years, spanning the range from high-resolution single-molecule experiments *in vitro* to the behavior of entire cell populations in living animals and even beyond. Furthermore, the introduction of new and smaller genetically encoded fluorescent reporters, such as the light-, oxygen-, or voltage-sensing domain of the plant blue light receptor phototropin (iLOV; [180]), should enable even more advanced fusions that potentially exhibit a wide spectrum of new properties and are not hampered by larger steric constraints of traditional FPs. Additionally, directed molecular engineering of endogenous proteins to modify or create unusual fluorescent properties holds promise as an emerging technique [181]. Underpinning all current and future achievements using FPs are the rapid advances in imaging technologies that emerge from the commercial sector [182–184]. Advanced new FP-related fluorophores coupled with highly sensitive imaging systems will afford new opportunities to examine age-old problems in biology and medicine.

CONCLUSIONS

The current thrust of FP development strategies centers on fine-tuning the current palette of blue-to-yellow FPs derived from the *Aequorea victoria* jellyfish while simultaneously developing monomeric FPs emitting in the orange to far-red regions of the visible light spectrum. Progress toward these goals has been substantial, and it is not inconceivable that near-infrared emitting FPs loom on the horizon. The latest efforts in jellyfish variants have resulted in new and improved monomeric probes for the blue, cyan, green, and yellow regions, whereas the search for a bright monomeric and fast-maturing red FP has yielded a host of excellent candidates spanning longer wavelengths. Continuing efforts in protein engineering of existing FPs, coupled with advanced new technologies, should further expand the color palette and ultimately provide proteins in every spectral class that mature rapidly and are bright and photostable. As the development of optical highlighters continues, FPs useful for optical marking should evolve toward brighter monomeric derivatives with high contrast that can be easily photoconverted and display a

wide spectrum of emission colors. For example, proteins capable of reversible photoactivation, red-to-green photoconversion, improved expression at elevated temperatures, and derivatives emitting in the far-red or near-infrared regions of the spectrum would be useful.

REFERENCES

- 1 Chudakov, D. M., Lukyanov, S., Lukyanov, K. A. (2005). Fluorescent proteins as a toolkit for *in vivo* imaging. *Trends Biotechnol* 23: 605–613.
- 2 Miyawaki, A., Nagai, T., Mizuno, H. (2005). Engineering fluorescent proteins. *Adv Biochem Eng Biotechnol* 95: 1–15.
- 3 Shaner, N. C., Steinbach, P. A., Tsien, R. Y. (2005). A guide to choosing fluorescent proteins. *Nat Methods* 2: 905–909.
- 4 Shaner, N. C., Patterson, G. H., Davidson, M. W. (2007). Advances in fluorescent protein technology. *J Cell Sci* 120: 4247–4260.
- 5 Zhang, J., Campbell, R. E., Ting, A. Y., Tsien, R. Y. (2002). Creating new fluorescent probes for cell biology. *Nat Rev Mol Cell Biol* 3: 906–918.
- 6 Meyer, T., Teruel, M. N. (2003). Fluorescence imaging of signaling networks. *Trends Cell Biol* 13: 101–106.
- 7 Miyawaki, A., Mizuno, H., Nagai, T., Sawano, A. (2003). Development of genetically encoded fluorescent indicators for calcium. *Methods Enzymol* 360: 202–225.
- 8 Zaccolo, M., Cesetti, T., Di Benedetto, G., Mongillo, M., Lissandron, V., Terrin, A., Zamparo, I. (2005). Imaging the cAMP-dependent signal transduction pathway. *Biochem Soc Trans* 33: 1323–1326.
- 9 Livet, J., Weissman, T. A., Kang, H. N., Draft, R. W., Lu, J., Bennis, R. A., Sanes, J. R., Lichtman, J. W. (2007). Transgenic strategies for combinatorial expression of fluorescent proteins in the nervous system. *Nature* 450: 56–62.
- 10 Day, R. N., Schaufele, F. (2005). Imaging molecular interactions in living cells. *Mol Endocrinol* 19: 1675–1686.
- 11 Lippincott-Schwartz, J., Patterson, G. H. (2003). Development and use of fluorescent protein markers in living cells. *Science* 300: 87–91.
- 12 Shimomura, O., Johnson, F. H., Saiga, Y. (1962). Extraction, purification and properties of Aequorin, a bioluminescent protein from luminous Hydromedusan, *Aequorea*. *J Cell Comp Physiol* 59 (1962): 223–239.
- 13 Chalfie, M., Tu, Y., Euskirchen, G., Ward, W. W., Prasher, D. C. (1994). Green fluorescent protein as a marker for gene expression. *Science* 263: 802–805.
- 14 Davenport, D., Nicol, J. A. C. (1955). Luminescence in Hydromedusae. *Proc R Soc Lond, B, Biol Sci* 144: 399–411.
- 15 Morin, J. G., Hastings, J. W. (1971). Energy transfer in a bioluminescent system. *J Cell Physiol* 77: 313–318.
- 16 Prasher, D. C., Eckenrode, V. K., Ward, W. W., Prendergast, F. G., Cormier, M. J. (1992). Primary structure of the *Aequorea victoria* green-fluorescent protein. *Gene* 111: 229–233.
- 17 Heim, R., Cubitt, A. B., Tsien, R. Y. (1995). Improved green fluorescence. *Nature* 373: 663–664.
- 18 Heim, R., Prasher, D. C., Tsien, R. Y. (1994). Wavelength mutations and posttranslational autoxidation of green fluorescent protein. *Proc Natl Acad Sci U S A* 91: 12501–12504.

- 19 Yang, T. T., Sinai, P., Green, G., Kitts, P. A., Chen, Y. T., Lybarger, L., Chervenak, R., Patterson, G. H., Piston, D. W., Kain, S. R. (1998). Improved fluorescence and dual color detection with enhanced blue and green variants of the green fluorescent protein. *J Biol Chem* **273**: 8212–8216.
- 20 Heim, R., Tsien, R. Y. (1996). Engineering green fluorescent protein for improved brightness, longer wavelengths and fluorescence resonance energy transfer. *Curr Biol* **6**: 178–182.
- 21 Wachter, R. M., Elsliger, M. A., Kallio, K., Hanson, G. T., Remington, S. J. (1998). Structural basis of spectral shifts in the yellow-emission variants of green fluorescent protein. *Structure* **6**: 1267–1277.
- 22 Matz, M. V., Fradkov, A. F., Labas, Y. A., Savitsky, A. P., Zaraisky, A. G., Markelov, M. L., Lukyanov, S. A. (1999). Fluorescent proteins from nonbioluminescent Anthozoa species. *Nat Biotechnol* **17**: 969–973.
- 23 Labas, Y. A., Gurskaya, N. G., Yanushevich, Y. G., Fradkov, A. F., Lukyanov, K. A., Lukyanov, S. A., Matz, M. V. (2002). Diversity and evolution of the green fluorescent protein family. *Proc Natl Acad Sci U S A* **99**: 4256–4261.
- 24 Matz, M. V., Lukyanov, K. A., Lukyanov, S. A. (2002). Family of the green fluorescent protein: journey to the end of the rainbow. *Bioessays* **24**: 953–959.
- 25 Masuda, H., Takenaka, Y., Yamaguchi, A., Nishikawa, S., Mizuno, H. (2006). A novel yellowish-green fluorescent protein from the marine copepod, *Chiridius poppei*, and its use as a reporter protein in HeLa cells. *Gene* **372**: 18–25.
- 26 Deheyn, D. D., Kubokawa, K., McCarthy, J. K., Murakami, A., Porrachia, M., Rouse, G. W., Holland, N. D. (2007). Endogenous green fluorescent protein (GFP) in amphioxus. *Biol Bull* **213**: 95–100.
- 27 Hopf, M., Gohring, W., Ries, A., Timpl, R., Hohenester, E. (2001). Crystal structure and mutational analysis of a perlecan-binding fragment of nidogen-1. *Nat Struct Biol* **8**: 634–640.
- 28 Jaiswal, J. K., Simon, S. M. (2004). Potentials and pitfalls of fluorescent quantum dots for biological imaging. *Trends Cell Biol* **14**: 497–504.
- 29 Giepmans, B. N. G., Adams, S. R., Ellisman, M. H., Tsien, R. Y. (2006). Review – the fluorescent toolbox for assessing protein location and function. *Science* **312**: 217–224.
- 30 Sapsford, K. E., Pons, T., Medintz, I. L., Mattoussi, H. (2006). Biosensing with luminescent semiconductor quantum dots. *Sensors* **6**: 925–953.
- 31 Michalet, X., Pinaud, F. F., Bentolila, L. A., Tsay, J. M., Doose, S., Li, J. J., Sundaresan, G., Wu, A. M., Gambhir, S. S., Weiss, S. (2005). Quantum dots for live cells, in vivo imaging, and diagnostics. *Science* **307**: 538–544.
- 32 McNamara, G., Boswell, C. (2006). PubSpectra; <http://home.earthlink.net/~pubspectra/>.
- 33 Dabbousi, B. O., Rodriguez-Viejo, J., Mikulec, F. V., Heine, J. R., Mattoussi, H., Ober, R., Jensen, K. F., Bawendi, M. G. (1997). (CdSe)ZnS core-shell quantum dots: synthesis and characterization of a size series of highly luminescent nanocrystallites. *J Phys Chem B* **101**: 9463–9475.
- 34 Wang, L., Jackson, W. C., Steinbach, P. A., Tsien, R. Y. (2004). Evolution of new nonantibody proteins via iterative somatic hypermutation. *Proc Natl Acad Sci U S A* **101**: 16745–16749.
- 35 Nguyen, A. W., Daugherty, P. S. (2005). Evolutionary optimization of fluorescent proteins for intracellular FRET. *Nat Biotechnol* **23**: 355–360.
- 36 Shaner, N. C., Campbell, R. E., Steinbach, P. A., Giepmans, B. N., Palmer, A. E., Tsien, R. Y. (2004). Improved monomeric red, orange and yellow fluorescent proteins derived from *Discosoma* sp. red fluorescent protein. *Nat Biotechnol* **22**: 1567–1572.
- 37 Ward, W. W. (2006). Biochemical and physical properties of green fluorescent protein. In: Chalfie, M., & Kain S. R. (Eds.), *Green Fluorescent Protein: Properties, Applications, and Protocols*, 2nd ed., Wiley-Interscience: New York, pp. 39–65.
- 38 Lakowicz, J. R. (2006). *Principles of Fluorescence Spectroscopy*, 3rd ed., Springer: New York.
- 39 Hazelwood, K. L., Olenych, S. G., Griffin, J. D., Cathcart, J. A., Davidson, M. W. (2007). Entering the portal: Understanding the digital image recorded through a microscope. In: Shorte, S. L., & Frischknecht, F. (Eds.), *Imaging Cellular and Molecular Biological Functions*. Springer: Berlin, pp. 3–43.
- 40 Henderson, J. N., Ai, H. W., Campbell, R. E., Remington, S. J. (2007). Structural basis for reversible photobleaching of a green fluorescent protein homologue. *Proc Natl Acad Sci U S A* **104**: 6672–6677.
- 41 Yang, F., Moss, L. G., Phillips, G. N., Jr. (1996). The molecular structure of green fluorescent protein. *Nat Biotechnol* **14**: 1246–1251.
- 42 Ormo, M., Cubitt, A. B., Kallio, K., Gross, L. A., Tsien, R. Y., Remington, S. J. (1996). Crystal structure of the *Aequorea victoria* green fluorescent protein. *Science* **273**: 1392–1395.
- 43 Weissleder, R. (2001). A clearer vision for in vivo imaging. *Nat Biotechnol* **19**: 316–317.
- 44 Zapata-Hommer, O., Griesbeck, O. (2003). Efficiently folding and circularly permuted variants of the Sapphire mutant of GFP. *BMC Biotechnol* **3**: 5.
- 45 Kogure, T., Karasawa, S., Araki, T., Saito, K., Kinjo, M., Miyawaki, A. (2006). A fluorescent variant of a protein from the stony coral *Montipora* facilitates dual-color single-laser fluorescence cross-correlation spectroscopy. *Nat Biotechnol* **24**: 577–581.
- 46 Xia, J., Kim, S. H., Macmillan, S., Truant, R. (2006). Practical three color live cell imaging by widefield microscopy. *Biol Proced Online* **8**: 63–68.
- 47 Chen, I., Ting, A. Y. (2005). Site-specific labeling of proteins with small molecules in live cells. *Curr Opin Biotechnol* **16**: 35–40.
- 48 Miller, L. W., Cornish, V. W. (2005). Selective chemical labeling of proteins in living cells. *Curr Opin Chem Biol* **9**: 56–61.
- 49 Gronemeyer, T., Godin, G., Johnsson, K. (2005). Adding value to fusion proteins through covalent labeling. *Curr Opin Biotechnol* **16**: 453–458.
- 50 Howarth, M., Takao, K., Hayashi, Y., Ting, A. Y. (2005). Targeting quantum dots to surface proteins in living cells with biotin ligase. *Proc Natl Acad Sci U S A* **102**: 7583–7588.
- 51 Griffin, B. A., Adams, S. R., Tsien, R. Y. (1998). Specific covalent labeling of recombinant protein molecules inside live cells. *Science* **281**: 269–272.
- 52 Keppler, A., Gendrezig, S., Gronemeyer, T., Pick, H., Vogel, H., Johnsson, K. (2003). A general method for the covalent

- labeling of fusion proteins with small molecules in vivo. *Nat Biotechnol* 21: 86–89.
- 53 Martin, B. R., Giepmans, B. N., Adams, S. R., Tsien, R. Y. (2005). Mammalian cell-based optimization of the biarsenical-binding tetracycline motif for improved fluorescence and affinity. *Nat Biotechnol* 23: 1308–1314.
- 54 Salih, A., Larkum, A., Cox, G., Kuhl, M., Hoegh-Guldberg, O. (2000). Fluorescent pigments in corals are photoprotective. *Nature* 408: 850–853.
- 55 Pedelacq, J. D., Cabantous, S., Tran, T., Terwilliger, T. C., Waldo, G. S. (2006). Engineering and characterization of a superfolder green fluorescent protein. *Nat Biotechnol* 24: 79–88.
- 56 Nagai, T., Ibata, K., Park, E. S., Kubota, M., Mikoshiba, K., Miyawaki, A. (2002). A variant of yellow fluorescent protein with fast and efficient maturation for cell-biological applications. *Nat Biotechnol* 20: 87–90.
- 57 Ai, H.-w., Shaner, N. C., Cheng, Z., Tsien, R. Y., Campbell, R. E. (2007). Exploration of new chromophore structures leads to the identification of improved blue fluorescent proteins. *Biochemistry* 46: 5904–5910.
- 58 Kremers, G. J., Goedhart, J., vanMunster, E. B., Gadella, T. W. J. (2006). Cyan and yellow super fluorescent proteins with improved brightness, protein folding, and FRET Forster radius. *Biochemistry* 45: 6570–6580.
- 59 Kremers, G. J., Goedhart, J., vandenHeuvel, D. J., Gerritsen, H. C., Gadella, T. W. J. (2007). Improved green and blue fluorescent proteins for expression in bacteria and mammalian cells. *Biochemistry* 46: 3775–3783.
- 60 Tsien, R. Y. (1998). The green fluorescent protein. *Annu Rev Biochem* 67: 509–544.
- 61 Wachter, R. M. (2007). Chromogenic cross-link formation in green fluorescent protein. *Acc Chem Res* 40: 120–127.
- 62 Gross, L. A., Baird, G. S., Hoffman, R. C., Baldrige, K. K., Tsien, R. Y. (2000). The structure of the chromophore within DsRed, a red fluorescent protein from coral. *Proc Natl Acad Sci U S A* 97: 11990–11995.
- 63 Zimmer, M. (2002). Green fluorescent protein (GFP): applications, structure, and related photophysical behavior. *Chem Rev* 102: 759–781.
- 64 Campbell, R. E., Tour, O., Palmer, A. E., Steinbach, P. A., Baird, G. S., Zacharias, D. A., Tsien, R. Y. (2002). A monomeric red fluorescent protein. *Proc Natl Acad Sci U S A* 99: 7877–7882.
- 65 Zacharias, D. A., Violin, J. D., Newton, A. C., Tsien, R. Y. (2002). Partitioning of lipid-modified monomeric GFPs into membrane microdomains of live cells. *Science* 296: 913–916.
- 66 Baird, G. S., Zacharias, D. A., Tsien, R. Y. (2000). Biochemistry, mutagenesis, and oligomerization of DsRed, a red fluorescent protein from coral. *Proc Natl Acad Sci U S A* 97: 11984–11989.
- 67 Verkhusha, V. V., Lukyanov, K. A. (2004). The molecular properties and applications of Anthozoa fluorescent proteins and chromoproteins. *Nat Biotechnol* 22: 289–296.
- 68 Zacharias, D. A., Tsien, R. Y. (2006). Molecular biology and mutation of green fluorescent protein. *Methods Biochem Anal* 47: 83–120.
- 69 Yarbrough, D., Wachter, R. M., Kallio, K., Matz, M. V., Remington, S. J. (2001). Refined crystal structure of DsRed, a red fluorescent protein from coral, at 2.0-Å resolution. *Proc Natl Acad Sci U S A* 98: 462–467.
- 70 Wall, M. A., Socolich, M., Ranganathan, R. (2000). The structural basis for red fluorescence in the tetrameric GFP homolog DsRed. *Nat Struct Biol* 7: 1133–1138.
- 71 Wiedenmann, J., Vallone, B., Renzi, F., Nienhaus, K., Ivanchenko, S., Rocker, C., Nienhaus, G. U. (2005). Red fluorescent protein eqFP611 and its genetically engineered dimeric variants. *J Biomed Opt* 10: 14003.
- 72 Karasawa, S., Araki, T., Yamamoto-Hino, M., Miyawaki, A. (2003). A green-emitting fluorescent protein from Galaxiidae coral and its monomeric version for use in fluorescence labeling. *J Biol Chem* 278: 34167–34171.
- 73 Karasawa, S., Araki, T., Nagai, T., Mizuno, H., Miyawaki, A. (2004). Cyan-emitting and orange-emitting fluorescent proteins as a donor/acceptor pair for fluorescence resonance energy transfer. *Biochem J* 381: 307–312.
- 74 Wiedenmann, J., Ivanchenko, S., Oswald, F., Schmitt, F., Rocker, C., Salih, A., Spindler, K. D., Nienhaus, G. U. (2004). EosFP, a fluorescent marker protein with UV-inducible green-to-red fluorescence conversion. *Proc Natl Acad Sci U S A* 101: 15905–15910.
- 75 Gurskaya, N. G., Verkhusha, V. V., Shcheglov, A. S., Staroverov, D. B., Chepurnykh, T. V., Fradkov, A. F., Lukyanov, S., Lukyanov, K. A. (2006). Engineering of a monomeric green-to-red photoactivatable fluorescent protein induced by blue light. *Nat Biotechnol* 24: 461–465.
- 76 Ando, R., Mizuno, H., Miyawaki, A. (2004). Regulated fast nucleocytoplasmic shuttling observed by reversible protein highlighting. *Science* 306: 1370–1373.
- 77 Ai, H.-w., Henderson, J. N., Remington, S. J., Campbell, R. E. (2006). Directed evolution of a monomeric, bright and photostable version of Clavularia cyan fluorescent protein: structural characterization and applications in fluorescence imaging. *Biochem J* 400: 531–540.
- 78 Fradkov, A. F., Verkhusha, V. V., Staroverov, D. B., Bulina, M. E., Yanushevich, Y. G., Martynov, V. I., Lukyanov, S., Lukyanov, K. A. (2002). Far-red fluorescent tag for protein labelling. *Biochem J* 368: 17–21.
- 79 Nienhaus, G. U., Nienhaus, K., Holzle, A., Ivanchenko, S., Renzi, F., Oswald, F., Wolff, M., Schmitt, F., Rocker, C., Vallone, B., Weidemann, W., Heilker, R., Nar, H., Wiedenmann, J. (2006). Photoconvertible fluorescent protein EosFP: biophysical properties and cell biology applications. *Photochem Photobiol* 82: 351–358.
- 80 Gavin, P., Devenish, R. J., Prescott, M. (2002). An approach for reducing unwanted oligomerisation of DsRed fusion proteins. *Biochem Biophys Res Commun* 298: 707–713.
- 81 Bulina, M. E., Verkhusha, V. V., Staroverov, D. B., Chudakov, D. M., Lukyanov, K. A. (2003). Hetero-oligomeric tagging diminishes non-specific aggregation of target proteins fused with anthozoa fluorescent proteins. *Biochem J* 371: 109–114.
- 82 Yanushevich, Y. G., Staroverov, D. B., Savitsky, A. P., Fradkov, A. F., Gurskaya, N. G., Bulina, M. E., Lukyanov, K. A., Lukyanov, S. A. (2002). A strategy for the generation of non-aggregating mutants of Anthozoa fluorescent proteins. *FEBS Lett* 511: 11–14.
- 83 Vinkenburg, J. L., Evers, T. H., Reulen, S. W., Meijer, E. W., Merckx, M. (2007). Enhanced sensitivity of FRET-based

- protease sensors by redesign of the GFP dimerization interface. *Chembiochem* 8: 1119–1121.
- 84 Ohashi, T., Galiacy, S. D., Briscoe, G., Erickson, H. P. (2007). An experimental study of GFP-based FRET, with application to intrinsically unstructured proteins. *Protein Sci* 16: 1429–1438.
- 85 Ghaemmaghami, S., Huh, W. K., Bower, K., Howson, R. W., Belle, A., Dephoure, N., O’Shea, E. K., Weissman, J. S. (2003). Global analysis of protein expression in yeast. *Nature* 425: 737–741.
- 86 Wallrabe, H., Periasamy, A. (2005). Imaging protein molecules using FRET and FLIM microscopy. *Curr Opin Biotechnol* 16: 19–27.
- 87 Millington, M., Grindlay, G. J., Altenbach, K., Neely, R. K., Kolch, W., Bencina, M., Read, N. D., Jones, A. C., Dryden, D. T., Magennis, S. W. (2007). High-precision FLIM-FRET in fixed and living cells reveals heterogeneity in a simple CFP-YFP fusion protein. *Biophys Chem* 127: 155–164.
- 88 Rizzo, M. A., Springer, G. H., Granada, B., Piston, D. W. (2004). An improved cyan fluorescent protein variant useful for FRET. *Nat. Biotechnol* 22: 445–449.
- 89 Shimomura, O. (1979). Structure of the chromophore of Aequorea green fluorescent protein. *FEBS Lett* 104: 220–222.
- 90 Cormack, B. P., Valdivia, R. H., Falkow, S. (1996). FACS-optimized mutants of the green fluorescent protein (GFP). *Gene* 173: 33–38.
- 91 Mena, M. A., Treynor, T. P., Mayo, S. L., Daugherty, P. S. (2006). Blue fluorescent proteins with enhanced brightness and photostability from a structurally targeted library. *Nat Biotechnol* 24: 1569–1571.
- 92 Griesbeck, O., Baird, G. S., Campbell, R. E., Zacharias, D. A., Tsien, R. Y. (2001). Reducing the environmental sensitivity of yellow fluorescent protein. Mechanism and applications. *J Biol Chem* 276: 29188–29194.
- 93 Shagin, D. A., Barsova, E. V., Yanushevich, Y. G., Fradkov, A. E., Lukyanov, K. A., Labas, Y. A., Semenova, T. N., Ugalde, J. A., Meyers, A., Nunez, J. M., Widder, E. A., Lukyanov, S. A., Matz, M. V. (2004). GFP-like proteins as ubiquitous metazoan superfamily: evolution of functional features and structural complexity. *Mol Biol Evol* 21: 841–850.
- 94 Dai, M., Fisher, H. E., Temirov, J., Kiss, C., Phipps, M. E., Pavlik, P., Werner, J. H., Bradbury, A. R. (2007). The creation of a novel fluorescent protein by guided consensus engineering. *Protein Eng Des Sel* 20: 69–79.
- 95 Treynor, T. P., Vizcarra, C. L., Nedelcu, D., Mayo, S. L. (2007). Computationally designed libraries of fluorescent proteins evaluated by preservation and diversity of function. *Proc Natl Acad Sci U S A* 104: 48–53.
- 96 Remington, S. J. (2006). Fluorescent proteins: maturation, photochemistry and photophysics. *Curr Opin Struct Biol* 16: 714–721.
- 97 Cubitt, A. B., Woollenweber, L. A., Heim, R. (1999). Understanding structure-function relationships in the Aequorea victoria green fluorescent protein. *Methods Cell Biol* 58: 19–30.
- 98 Stephens, D. J., Allan, V. J. (2003). Light microscopy techniques for live cell imaging. *Science* 300: 82–86.
- 99 Khodjakov, A., Rieder, C. L. (2006). Imaging the division process in living tissue culture cells. *Methods* 38: 2–16.
- 100 Subach, O. M., Gundorov, I. S., Yoshimura, M., Subach, F. V., Zhang, J. H., Gruenwald, D., Souslova, E. A., Chudakov, D. M., Verkhusha, V. V. (2008). Conversion of red fluorescent protein into a bright blue probe. *Chem Biol* 59: 1116–1124.
- 101 Miyawaki, A., Llopis, J., Heim, R., McCaffery, J. M., Adams, J. A., Ikura, M., Tsien, R. Y. (1997). Fluorescent indicators for Ca²⁺ based on green fluorescent proteins and calmodulin. *Nature* 388: 882–887.
- 102 Day, R. N., Booker, C. F., Periasamy, A. (2008). The characterization of an improved donor fluorescent protein for Förster resonance energy transfer microscopy. *J Biomed Optics*.
- 103 Rizzo, M. A., Piston, D. W. (2005). High-contrast imaging of fluorescent protein FRET by fluorescence polarization microscopy. *Biophys J* 88: L14–L16.
- 104 Kremers, G. J., Goedhart, J., van Munster, E. B., Gadella, T. W. Jr. (2006). Cyan and yellow super fluorescent proteins with improved brightness, protein folding, and FRET Förster radius. *Biochemistry* 45: 6570–6580.
- 105 Richards, B., Zharkikh, L., Hsu, F., Dunn, C., Kamb, A., Teng, D. H. (2002). Stable expression of Anthozoa fluorescent proteins in mammalian cells. *Cytometry* 48: 106–112.
- 106 Luo, W. X., Cheng, T., Guan, B. Q., Li, S. W., Miao, J., Zhang, J., Xia, N. S. (2006). Variants of green fluorescent protein GFP_{xm}. *Mar Biotechnol* 8: 560–566.
- 107 Ai, H.-w., Olenych, S. G., Wong, P., Davidson, M. W., Campbell, R. E. (2008). Hue-shifted monomeric variants of Clavularia cyan fluorescent protein: identification of the molecular determinants of color and applications in fluorescence imaging. *BMC Biol* 6: 13.
- 108 Cormier, M. J., Eckroade, C. B. (1962). Studies on the bioluminescence of *Renilla reniformis*. III. Some biochemical comparisons of the system to other *Renilla* species and determinations of the spectral energy distributions. *Biochim Biophys Acta* 64: 340–344.
- 109 Miyawaki, A. (2002). Green fluorescent protein-like proteins in reef Anthozoa animals. *Cell Struct Funct* 27: 343–347.
- 110 Cornea, A., Conn, P. M. (2002). Measurement of changes in fluorescence resonance energy transfer between gonadotropin-releasing hormone receptors in response to agonists. *Methods* 27: 333–339.
- 111 Sturman, D. A., Shakiryanova, D., Hewes, R. S., Deitcher, D. L., Levitan, E. S. (2006). Nearly neutral secretory vesicles in *Drosophila* nerve terminals. *Biophys J* 90: L45–47.
- 112 Tavare, J. M., Fletcher, L. M., Welsh, G. I. (2001). Using green fluorescent protein to study intracellular signalling. *J Endocrinol* 170: 297–306.
- 113 Gurskaya, N. G., Savitsky, A. P., Yanushevich, Y. G., Lukyanov, S. A., Lukyanov, K. A. (2001). Color transitions in coral’s fluorescent proteins by site-directed mutagenesis. *BMC Biochem* 2: 6.
- 114 Sakaue-Sawano, A., Kurokawa, H., Morimura, T., Hanyu, A., Hama, H., Osawa, H., Kashiwagi, S., Fukami, K., Miyata, T., Miyoshi, H., Imamura, T., Ogawa, M., Masai, H., Miyawaki, A. (2008). Visualizing spatiotemporal dynamics of multicellular cell-cycle progression. *Cell* 132: 487–498.
- 115 Shaner, N. C., Lin, M. Z., McKeown, M. R., Steinbach, P. A., Hazelwood, K. L., Davidson, M. W., Tsien, R. Y.

- (2008). Improving the photostability of bright monomeric orange and red fluorescent proteins. *Nat Methods* 5: 545–551.
- 116 Ip, D. T., Chan, S. H., Allen, M. D., Bycroft, M., Wan, D. C., Wong, K. B. (2004). Crystallization and preliminary crystallographic analysis of a novel orange fluorescent protein from the Cnidaria tube anemone *Cerianthus* sp. *Acta Crystallogr D Biol Crystallogr* 60: 340–341.
- 117 Rizzo, M. A., Piston, D. W. (2005). Fluorescent protein tracking and detection. In: Goldman, R. D. & Spector D. L. (Eds.), *Live Cell Imaging: A Laboratory Manual*. Cold Spring Harbor Laboratory Press: Cold Spring Harbor: 3–23.
- 118 Merzlyak, E. M., Goedhart, J., Shcherbo, D., Bulina, M. E., Shcheglov, A. S., Fradkov, A. F., Gaintzeva, A., Lukyanov, K. A., Lukyanov, S., Gadella, T. W., Chudakov, D. M. (2007). Bright monomeric red fluorescent protein with an extended fluorescence lifetime. *Nat Methods* 4: 555–557.
- 119 Patterson, G. H. (2004). A new harvest of fluorescent proteins. *Nat Biotechnol* 22: 1524–1525.
- 120 Tsiens, R. Y. (2005). Building and breeding molecules to spy on cells and tumors. *FEBS Lett* 579: 927–932.
- 121 Wang, C. L., Yang, D. C., Wabl, M. (2004). Directed molecular evolution by somatic hypermutation. *Protein Eng Des Sel* 17: 659–664.
- 122 Shkrob, M. A., Yanushevich, Y. G., Chudakov, D. M., Gurskaya, N. G., Labas, Y. A., Poponov, S. Y., Mudrik, N. N., Lukyanov, S., Lukyanov, K. A. (2005). Far-red fluorescent proteins evolved from a blue chromoprotein from *Actinia equina*. *Biochem J* 392: 649–654.
- 123 Gurskaya, N. G., Fradkov, A. F., Tersikh, A., Matz, M. V., Labas, Y. A., Martynov, V. I., Yanushevich, Y. G., Lukyanov, K. A., Lukyanov, S. A. (2001). GFP-like chromoproteins as a source of far-red fluorescent proteins. *FEBS Lett* 507: 16–20.
- 124 Wiedenmann, J., Schenk, A., Rocker, C., Girod, A., Spindler, K. D., Nienhaus, G. U. (2002). A far-red fluorescent protein with fast maturation and reduced oligomerization tendency from *Entacmaea quadricolor* (Anthozoa, Actinaria). *Proc Natl Acad Sci U S A* 99: 11646–11651.
- 125 Schenk, A., Ivanchenko, S., Rocker, C., Wiedenmann, J., Nienhaus, G. U. (2004). Photodynamics of red fluorescent proteins studied by fluorescence correlation spectroscopy. *Biophys J* 86: 384–394.
- 126 Kredel, S., Oswald, F., Nienhaus, K., Deuschle, K., Rocker, C., Wolff, M., Heilker, R., Nienhaus, G. U., Wiedenmann, J. (2009). A monomeric eqFP611 variant for labeling of subcellular structures. *PLoS ONE* 3.
- 127 Lukyanov, K. A., Fradkov, A. F., Gurskaya, N. G., Matz, M. V., Labas, Y. A., Savitsky, A. P., Markelov, M. L., Zaraisky, A. G., Zhao, X., Fang, Y., Tan, W., Lukyanov, S. A. (2000). Natural animal coloration can be determined by a nonfluorescent green fluorescent protein homolog. *J Biol Chem* 275: 25879–25882.
- 128 Shcherbo, D., Merzlyak, E. M., Chepurnykh, T. V., Fradkov, A. F., Ermakova, G. V., Solovieva, E. A., Lukyanov, K. A., Bogdanova, E. A., Zaraisky, A. G., Lukyanov, S., Chudakov, D. M. (2007). Bright far-red fluorescent protein for whole-body imaging. *Nat Methods* 4: 741–746.
- 129 Lukyanov, K. A., Chudakov, D. M., Lukyanov, S., Verkhusha, V. V. (2005). Innovation: Photoactivatable fluorescent proteins. *Nat Rev Mol Cell Biol* 6: 885–891.
- 130 Ando, R., Hama, H., Yamamoto-Hino, M., Mizuno, H., Miyawaki, A. (2002). An optical marker based on the UV-induced green-to-red photoconversion of a fluorescent protein. *Proc Natl Acad Sci U S A* 99: 12651–12656.
- 131 Patterson, G. H., Lippincott-Schwartz, J. (2002). A photoactivatable GFP for selective photolabeling of proteins and cells. *Science* 297: 1873–1877.
- 132 Chudakov, D. M., Belousov, V. V., Zaraisky, A. G., Novoselov, V. V., Staroverov, D. B., Zorov, D. B., Lukyanov, S., Lukyanov, K. A. (2003). Kindling fluorescent proteins for precise in vivo photolabeling. *Nat Biotechnol* 21: 191–194.
- 133 Betzig, E., Patterson, G. H., Sougrat, R., Lindwasser, O. W., Olenych, S., Bonifacino, J. S., Davidson, M. W., Lippincott-Schwartz, J., Hess, H. F. (2006). Imaging intracellular fluorescent proteins at nanometer resolution. *Science* 313: 1642–1645.
- 134 Schwentker, M. A., Bock, H., Hofmann, M., Jakobs, S., Bewersdorf, J., Eggeling, C., Hell, S. W. (2007). Wide-field subdiffraction RESOLFT microscopy using fluorescent protein photoswitching. *Microsc Res Tech* 70: 269–280.
- 135 Verkhusha, V. V., Sorkin, A. (2005). Conversion of the monomeric red fluorescent protein into a photoactivatable probe. *Chem Biol* 12: 279–285.
- 136 Chudakov, D. M., Verkhusha, V. V., Staroverov, D. B., Souslova, E. A., Lukyanov, S., Lukyanov, K. A. (2004). Photoswitchable cyan fluorescent protein for protein tracking. *Nat Biotechnol* 22: 1435–1439.
- 137 Tsutsui, H., Karasawa, S., Shimizu, H., Nukina, N., Miyawaki, A. (2005). Semi-rational engineering of a coral fluorescent protein into an efficient highlighter. *EMBO Rep* 6: 233–238.
- 138 Ivanchenko, S., Rocker, C., Oswald, F., Wiedenmann, J., Nienhaus, G. U. (2005). Targeted green-red photoconversion of EosFP, a fluorescent marker protein. *J Biol Phys* 31: 249–259.
- 139 Habuchi, S., Tsutsui, H., Kochaniak, A. B., Miyawaki, A., van Oijen, A. M. (2008). mKikGR, a monomeric photo-switchable fluorescent protein. *PLoS ONE* 3: e3944.
- 140 McKinney, S. A., Murphy, C. S., Hazelwood, K. L., Davidson, M. W., Looger, L. L. (2008). A bright and photostable photoconvertible fluorescent protein for fusion tags. *Nature Meth* 6.
- 141 Mizuno, H., Mal, T. K., Tong, K. I., Ando, R., Furuta, T., Ikura, M., Miyawaki, A. Photo-induced peptide cleavage in the green-to-red conversion of a fluorescent protein. *Mol Cell* 12: 1051–1058.
- 142 Nienhaus, K., Nienhaus, G. U., Wiedenmann, J., Nar, H. (2005). Structural basis for photo-induced protein cleavage and green-to-red conversion of fluorescent protein EosFP. *Proc Natl Acad Sci U S A* 102: 9156–9159.
- 143 Cinelli, R. A. G., Pellegrini, V., Ferrari, A., Faraci, P., Nifosi, R., Tyagi, M., Giacca, M., Beltram, F. (2001). Green fluorescent proteins as optically controllable elements in bioelectronics. *Appl Phys Lett* 79: 3353–3355.
- 144 McAnaney, T. B., Zeng, W., Doe, C. F. E., Bhanji, N., Wakelin, S., Pearson, D. S., Abbyad, P., Shi, X. H., Boxer, S. G., Bagshaw, C. R. (2005). Protonation, photobleaching, and photoactivation of yellow fluorescent protein (YFP 10C): A unifying mechanism. *Biochemistry* 44: 5510–5524.

- 145 Dickson, R. M., Cubitt, A. B., Tsien, R. Y., Moerner, W. E. (1997). On/off blinking and switching behaviour of single molecules of green fluorescent protein. *Nature* **388**: 355–358.
- 146 Habuchi, S., Cotlet, M., Gensch, T., Bednarz, T., Haber-Pohlmeier, S., Rozenski, J., Dirix, G., Michiels, J., Vanderleyden, J., Heberle, J., De Schryver, F. C., Hofkens, J. (2005). Evidence for the isomerization and decarboxylation in the photoconversion of the red fluorescent protein DsRed. *J Am Chem Soc* **127**: 8977–8984.
- 147 Chudakov, D. M., Feofanov, A. V., Mudrik, N. N., Lukyanov, S., Lukyanov, K. A. (2003). Chromophore environment provides clue to “kindling fluorescent protein” riddle. *J Biol Chem* **278**: 7215–7219.
- 148 Andresen, M., Wahl, M. C., Stiel, A. C., Grater, F., Schafer, L. V., Trowitzsch, S., Weber, G., Eggeling, C., Grubmuller, H., Hell, S. W., Jakobs, S. (2005). Structure and mechanism of the reversible photoswitch of a fluorescent protein. *Proc Natl Acad Sci U S A* **102**: 13070–13074.
- 149 Andresen, M., Stiel, A. C., Trowitzsch, S., Weber, G., Eggeling, C., Wahl, M. C., Hell, S. W., Jakobs, S. (2007). Structural basis for reversible photoswitching in Dronpa. *Proc Natl Acad Sci U S A* **104**: 13005–13009.
- 150 Henderson, J. N., Remington, S. J. (2006). The kindling fluorescent protein: a transient photoswitchable marker. *Physiology (Bethesda)* **21**: 162–170.
- 151 Stiel, A. C., Trowitzsch, S., Weber, G., Andresen, M., Eggeling, C., Hell, S. W., Jakobs, S., Wahl, M. C. (2007). 1.8 Å bright-state structure of the reversibly switchable fluorescent protein Dronpa guides the generation of fast switching variants. *Biochem J* **402**: 35–42.
- 152 Baird, G. S., Zacharias, D. A., Tsien, R. Y. (1999). Circular permutation and receptor insertion within green fluorescent proteins. *Proc Natl Acad Sci U S A* **96**: 11241–11246.
- 153 Topell, S., Hennecke, J., Glockshuber, R. (1999). Circularly permuted variants of the green fluorescent protein. *FEBS Lett* **457**: 283–289.
- 154 Kozak, M. (1987). An analysis of 5′-noncoding sequences from 699 vertebrate messenger RNAs. *Nucleic Acids Res* **15**: 8125–8148.
- 155 Fernandez-Suarez, M., Ting, A. Y. (2008). Fluorescent probes for super-resolution imaging in living cells. *Nat Rev Mol Cell Biol* **9**: 929–943.
- 156 Lippincott-Schwartz, J., Manley, S. (2009). Putting super-resolution fluorescence microscopy to work. *Nat Methods* **6**: 21–23.
- 157 Seefeldt, B., Kasper, R., Seidel, T., Tinnfeld, P., Dietz, K. J., Heilemann, M., Sauer, M. (2008). Fluorescent proteins for single-molecule fluorescence applications. *J Biophoton* **1**: 74–82.
- 158 Douglass, A. D., Vale, R. D. (2008). Single-molecule imaging of fluorescent proteins. *Methods Cell Biol* **85**: 113–125.
- 159 Miyawaki, A. (2005). Innovations in the imaging of brain functions using fluorescent proteins. *Neuron* **48**: 189–199.
- 160 Querido, E., Chartrand, P. (2008). Using fluorescent proteins to study mRNA trafficking in living cells. *Methods Cell Biol* **85**: 273–292.
- 161 Dahm, R., Zeitelhofer, M., Gotze, B., Kiebler, M. A., Macchi, P. (2008). Visualizing mRNA localization and local protein translation in neurons. *Methods Cell Biol* **85**: 293–327.
- 162 Piston, D. W., Kremers, G. J. (2007). Fluorescent protein FRET: the good, the bad and the ugly. *Trends Biochem Sci* **32**: 407–414.
- 163 Miyawaki, A. (2003). Visualization of the spatial and temporal dynamics of intracellular signaling. *Dev Cell* **4**: 295–305.
- 164 Lalonde, S., Ehrhardt, D. W., Frommer, W. B. (2005). Shining light on signaling and metabolic networks by genetically encoded biosensors. *Curr Opin Plant Biol* **8**: 574–581.
- 165 Ciruela, F. (2008). Fluorescence-based methods in the study of protein-protein interactions in living cells. *Curr Opin Biotechnol* **19**: 338–343.
- 166 Pflieger, K. D. G., Eidne, K. A. (2006). Illuminating insights into protein-protein interactions using bioluminescence resonance energy transfer (BRET). *Nat Methods* **3**: 165–174.
- 167 Xu, X. D., Soutto, M., Xie, Q., Servick, S., Subramanian, C., von Arnim, A. G., Johnson, C. H. (2007). Imaging protein interactions with bioluminescence resonance energy transfer (BRET) in plant and mammalian cells and tissues. *Proc Natl Acad Sci U S A* **104**: 10264–10269.
- 168 Dixit, R., Cyr, R., Gilroy, S. (2006). Using intrinsically fluorescent proteins for plant cell imaging. *Plant J* **45**: 599–615.
- 169 Mathur, J. (2007). The illuminated plant cell. *Trends Plant Sci* **12**: 506–513.
- 170 Haseloff, J., Siemering, K. R. (2006). The uses of green fluorescent protein in plants. *Methods Biochem Anal* **47**: 259–284.
- 171 Kerppola, T. K. (2006). Visualization of molecular interactions by fluorescence complementation. *Nat Rev Mol Cell Biol* **7**: 449–456.
- 172 Kerppola, T. K. (2008). Biomolecular fluorescence complementation (BiFC) analysis as a probe of protein interactions in living cells. *Annu Rev Biophys* **37**: 465–487.
- 173 Langowski, J. (2008). Protein-protein interactions determined by fluorescence correlation spectroscopy. *Methods Cell Biol* **85**: 471–484.
- 174 Hoffman, R. M., Yang, M. (2006). Whole-body imaging with fluorescent proteins. *Nat Protoc* **1**: 1429–1438.
- 175 Barth, A. L. (2007). Visualizing circuits and systems using transgenic reporters of neural activity. *Curr Opin Neurobiol* **17**: 567–571.
- 176 Hadjantonakis, A. K., Dickinson, M. E., Fraser, S. E., Papaioannou, V. E. (2003). Technicolour transgenics: Imaging tools for functional genomics in the mouse. *Nat Rev Genet* **4**: 613–625.
- 177 Michnick, S. W., Ear, P. H., Manderson, E. N., Remy, I., Stefan, E. (2007). Universal strategies in research and drug discovery based on protein-fragment complementation assays. *Nat Rev Drug Discov* **6**: 569–582.
- 178 Wolff, M., Wiedenmann, J., Nienhaus, G. U., Valler, M., Heilker, R. (2006). Novel fluorescent proteins for high-content screening. *Drug Discov Today* **11**: 1054–1060.
- 179 Gaietta, G. M., Giepmans, B. N. G., Deerinck, T. J., Smith, W. B., Ngan, L., Llopis, J., Adams, S. R., Tsien, R. Y., Ellisman, M. H. (2006). Golgi twins in late mitosis revealed by genetically encoded tags for live cell imaging and correlated electron microscopy. *Proc Natl Acad Sci U S A* **103**: 17777–17782.

- 180 Chapman, S., Faulkner, C., Kaiserli, E., Garcia-Mata, C., Savenkov, E. I., Roberts, A. G., Oparka, K. J., Christie, J. M. (2008). The photoreversible fluorescent protein iLOV outperforms GFP as a reporter of plant virus infection. *Proc Natl Acad Sci U S A* **105**: 20038–20043.
- 181 Berndt, A., Yizhar, O., Gunaydin, L. A., Hegemann, P., Deisseroth, K. (2008). Bi-stable neural state switches. *Nat Neurosci* **12**(2) 229–234.
- 182 Sluder, G., Wolf D. W. (Eds.) (2007). *Digital Microscopy*, 3rd ed., Elsevier: New York.
- 183 Shorte, S. L., Frischknecht, F. (Eds.) (2007). *Imaging Cellular and Molecular Biological Functions*. Springer-Verlag: Berlin.
- 184 Tsien, R. Y. (2003). Imagining imaging's future. *Nat Rev Mol Cell Biol*: Ss16–Ss21.
- 185 Cubitt, A. B., Heim, R., Adams, S. R., Boyd, A. E., Gross, L. A., Tsien, R. Y. (1995). Understanding, improving and using green fluorescent proteins. *Trends Biochem Sci* **20**: 448–455.
- 186 Miyawaki, A., Griesbeck, O., Heim, R., Tsien, R. Y. (1999). Dynamic and quantitative Ca²⁺ measurements using improved cameleons. *Proc Natl Acad Sci U S A* **96**: 2135–2140.
- 187 Ai, H.-w., Hazelwood, K. L., Davidson, M. W., Campbell, R. E. (2008). Fluorescent protein FRET pairs for ratio-metric imaging of dual biosensors. *Nat Methods* **5**: 401–403.
- 188 Bevis, B. J., Glick, B. S. (2002). Rapidly maturing variants of the *Discosoma* red fluorescent protein (DsRed). *Nat Biotechnol* **20**: 83–87.